THE COUPLED BOUNDARY LAYERS AND AIR-SEA TRANSFER EXPERIMENT IN LOW WINDS (CBLAST-LOW)

BY JAMES EDSON, TIMOTHY CRAWFORD*, JERRY CRESCENTI, TOM FARRAR, NELSON FREW, GREG GERBI, COSTAS HELMIS, TIHOMIR HRISTOV, DJAMAL KHELIF, ANDREW JESSUP, HAF JONSSON, MING LI, LARRY MAHRT, WADE MCGILLIS, ALBERT PLUEDDEMANN, LIAN SHEN, ERIC SKYLLINGSTAD, TIM STANTON, PETER SULLIVAN, JIELUN SUN, JOHN TROWBRIDGE, DEAN VICKERS, SHOUPING WANG, QING WANG, ROBERT WELLER, JOHN WILKIN, D.K.P. YUE, AND CHRIS ZAPPA

AFFILIATIONS: EDSON – University of Connecticut, Groton, Connecticut; CRESCENTI – FPL Energy, Juno Beach, Florida; FARRAR, FREW, GERBI, PLUEDDEMANN, TROWBRIDGE, AND WELLER – Woods Hole Oceanographic Institution, Woods Hole, Massachusetts; HELMIS – University of Athens, Athens, Greece; HRISTOV AND SHEN – Johns Hopkins University, Baltimore, Maryland; KHELIF – University of California, Irvine, California; JESSUP – Applied Physics Laboratory, University of Washington, Seattle, Washington; JONSSON – CIRPAS, Monterey, California; LI – University of Maryland, College Park, Maryland; MAHRT, SKYLLINGSTAD, AND VICKERS, Oregon State University, Corvallis, Oregon; MCGILLIS AND ZAPPA – Lamont Doherty Earth Observatory, Columbia University, Palisades, New York; STANTON AND Q. WANG – Naval Postgraduate School, Monterey, California; SULLIVAN AND SUN, National Center for Atmospheric Research, Boulder, Colorado; S. WANG – Naval Research Laboratory, Monterey, California; WILKIN – Rutgers University, New Brunswick, New Jersey; YUE – Massachusetts Institute of Technology, Cambridge, Massachusetts.

CORRESPONDING AUTHOR: James Edson, University of Connecticut, Department of Marine Sciences, 1080 Shennecosset Road, Groton, CT 06340

E-mail: james.edson@uconn.edu

Observations from a suite of platforms deployed in the coastal ocean south of Martha's Vineyard are combined with numerical models and simulations to investigate the processes that couple the atmosphere and ocean at low to moderate wind conditions.

The need to better understand and model the interdependence of the ocean and atmosphere has long been recognized in the climate and weather communities. Work has been carried out to investigate how the upper ocean responds to the atmosphere, leading to 1-D models of upper ocean response to the atmosphere (e.g., Kraus and Turner, 1967; Price et al., 1986) and more recently to fully three dimensional (3-D) ocean boundary layer (OBL) models employing closure schemes similar to those used in the atmospheric boundary layer (ABL; e.g. Mellor and Yamada, 1982; Large et al., 1994). However, progress on fully two-way coupled models has been slower, particularly on shorter, weather-related, timescales.

There are a number of reasons for this, e.g., the dynamics of the coupled marine boundary layers are driven by a myriad of processes (Fig. 1), observations of the marine environment lacked the necessary temporal and spatial resolution, oceanographic models of the ocean surface were not sufficiently advanced, parameterizations required to couple the models contained too much uncertainty, and lack of evidence that the inclusion of a dynamic ocean would improve 3-5 day atmospheric forecasts. Now, however, there is increasing evidence that fully coupled models can often improve marine forecasts over shorter time scales. This is true in coastal regimes where air-land-sea contrasts drive mesoscale atmospheric circulations, fog formation, coastal upwelling, and tidal mixing. This is also true of hurricane intensity forecasts. Progress now underway to improve coupled models stems from 1) significant improvements in ocean models over the past decade and 2) observing initiatives that provide data needed to initialize

these models and assess the success of different parameterizations. This article and the companion that follow focus on a recent program designed to improve coupled models in both low and extreme wind conditions.

CBLAST. The Coupled Boundary Layer and Air-Sea Transfer (CBLAST) program was a major Office of Naval Research (ONR) sponsored investigation to look at two extremes of the marine environment where coupled ocean-atmosphere processes have a clear impact on both boundary layers. At one extreme, investigators in the CBLAST-Hurricane component are attempting to improve hurricane intensity forecasts and our understanding of the ocean's response as described in the companion articles by Chen et al. (2006) and Black et al. (2006).

CBLAST-LOW was designed to investigate coupled boundary layer (CBL) processes at the low-wind extreme where the processes may be driven or strongly modulated by thermal forcing in the surface ocean and lower atmosphere. The focus was on conditions ranging from where wind stress is negligible and thermal forcing dominates up to wind speeds where wave breaking and Langmuir circulations play a significant role in the exchange processes. Additionally, as CBLAST-LOW developed, it became apparent that additional wave-driven processes could not be ignored, including the impact of ocean swell from distant storms on coupled boundary layer structure.

The goal of CBLAST-LOW is therefore to improve our understanding of the processes that couple the marine boundary layers under these conditions using observations, numerical simulations and models. The ultimate goal is to incorporate new and/or improved parameterization of these processes in coupled models to improve marine forecasts of wind, waves and currents. The article begins by briefly describing the observational and modeling

components. It then provides examples of how these components are being combined to meet these objectives.

OBSERVATIONAL COMPONENTS. CBLAST-LOW was conducted during intensive operating periods (IOPs) in the summers of 2001 through 2003 in the Atlantic Ocean south of Martha's Vineyard and shown in Fig. 2. A wide range of temporal and spatial scales was sampled by use of an array of fixed and mobile platforms; including an offshore tower, surface moorings, aircraft, ships, rawinsondes, satellites, and a coastal observatory.

Air-Sea Interaction Tower. Marine researchers have long sought stable ocean platforms that would allow studies of turbulent air-sea exchanges. A primary technological objective of the CBLAST-LOW program was to build an Air-Sea Interaction Tower (ASIT) to enable long-duration studies of the processes on both sides of the air-sea interface. ASIT is a low profile, fixed structure that minimizes flow distortion and removes the need for motion correction.

The ASIT, located 3.2 km south of Martha's Vineyard in 15-m water depth, was completed in the summer of 2002. It is attached by cable to the Martha's Vineyard Coastal Observatory (MVCO), which provides power (4 kW) and a high-bandwidth (1 Gbyte) data link (Austin et al., 2002). The MVCO provides a meteorological mast on the beach and a bottom-mounted seanode as shown in Fig. 3.

Atmospheric sensors at fixed heights and on a vertical profiler were deployed on the ASIT during the 2003 IOP to directly measure the vertical exchange of momentum, heat and moisture that couple the boundary layers. The air-side components included sensors to measure the mean

and turbulent wind velocity, air temperature, specific humidity, and pressure; as well as precipitation, solar and infrared radiation, sea surface temperature, and wave height. (Fig. 4a).

Oceanographic sensors were deployed beneath the surface to make similar measurements of currents, temperature, and salinity. Turbulence sensors were mounted on horizontal booms spanning two legs of the ASIT (Fig. 4b) to provide direct estimates of momentum and heat exchange just below the surface. To our knowledge, this represents the first successful attempt to measure directly and simultaneously the heat and momentum exchange on both sides of the air-sea interface. All fixed turbulent exchange sensors are summarized in Table 1.

Surface mooring array. Surface mooring arrays were deployed in the CBLAST-LOW operating area south of Martha's Vineyard during all 3 field campaigns. Two moorings were deployed 20 and 40 km offshore in 2001 to collect records of surface forcing and temporal evolution of vertical ocean structure (Pritchard and Weller, 2005). These records revealed the significant impact of synoptic weather systems on regional oceanographic variability. To resolve this variability and examine the ability of regional atmospheric and ocean models to simulate it, a six-surface mooring array was deployed from late June to early September 2002 spanning a 20 km wide by 40 km long region south of the Vineyard (Wilkin, 2006).

During the August 2003 IOP, surface meteorological and upper ocean measurements were collected from 15 instrumented surface moorings (Fig. 2). Five "heavy" moorings supported surface meteorological and in the ocean temperature, salinity, and velocity sensors with 2-m vertical resolution. The "light" moorings supported temperature sensors with 2-m vertical resolution. The goal was to obtain a continuous 3-D picture of the oceanic temperature field to investigate mesoscale variability in upper ocean dynamics and air-sea coupling.

***Ship-based surveys*.** Ship-based operations where conducted during all three summers. During the August 2003 IOP surface meteorological and upper ocean measurements were collected by the *F/V Nobska* during four survey cruises. The *Nobska* deployed and tracked 5 drifting buoys each outfitted with a high resolution (0.5m) vertical temperature array and two levels of salinity measurements.

The *Nobska* also towed a similar vertical array with fast response temperature or temperature/salinity sensors through targeted surface features and routinely made CTD (conductivity, temperature, depth) profiles. The ship carried upward and downward looking IR radiometers to estimate the sea surface temperature (SST), direct covariance flux system (DCFS), and shortwave and longwave radiometers to make continuous measurements of the momentum, heat, mass, and radiative fluxes during the oceanic surveys (Fig. 5a).

Surfactant film distributions were surveyed during the 2002 and 2003 IOPS using a new survey tool, SCIMS (Slick Chemical Identification and Measurement System). SCIMS is a semi-autonomous mobile instrument platform deployed off the *R/V Asterias* that detects the presence of surface microlayer films and allows mapping of their spatial and temporal distributions (Fig. 5b). Measurements to characterize surface films were carried out under different wind stress conditions in order to determine the patchiness of surface film distributions on scales ranging from 10m to 5 km.

Aircraft Measurements. Three aircraft participated in CBLAST-LOW: a Cessna Skymaster providing IR remote sensing and two aircraft that provided measurements of the mean and turbulent structure of the ABL. NOAA's Long-EZ airplane (N3R) provided measurements of

atmospheric turbulence from 10-m to the top of the boundary layer. The aircraft is instrumented with a suite of sensors to measure wind velocity, pressure, air temperature, humidity, and net (long and short) radiation. Direct covariance fluxes of heat, moisture, and momentum are derived using the approach described by Vickers and Mahrt (2005). Results from the 2001 IOP are reported in Grimmett et al. (2006).

The CIRPAS Pelican is similarly instrumented aircraft to measure atmospheric turbulence, mean variables, and remotely sensed measurements of sea-surface characteristics. The Pelican was used to map atmospheric boundary layer structure in support of the CBLAST-Low 2003 investigations.

IR Remote Sensing. Measurements of SST variability were made in 2001 from the Long-EZ and in 2002 and 2003 from the Cessna Skymaster. The Skymaster supported a state-of-the-art, high spatial resolution IR imaging system providing calibrated, sky-corrected imagery of SST. A downward-looking digital video camera was used to characterize the sea surface conditions. The surveys in 2002 and 2003, coordinated with the ship surveys, quantified the horizontal mesoscale variability in the SST field (Fig. 6) and investigated links between SST variability, ABL structure, and air-sea fluxes.

Nantucket Field Site. The Nantucket Island site, about 50 km southwest of the ASIT, supported rawinsonde launches (Loran-C sondes) every 4-6 hours, continuous sampling of the lower boundary layer from a SODAR, a ceiliometer to measure cloud base height, and turbulence and mean measurements from a flux tower. The measurement periods were between July 31 and August 23 in 2002 and from July 22 to August 27 in 2003.

COUPLED MODELS. One of the main objectives of CBLAST-Low project is to improve surface and boundary layer parameterizations in Naval Research Laboratory's Coupled Ocean/Atmosphere Mesoscale Prediction System (COAMPS®) for low-wind conditions. Real-time COAMPS® weather forecasts provided for the CBLAST-Low field experiment are being used with the measurements to evaluate the model physics and investigate the impacts of air-sea interaction on the mesoscale weather prediction.

The COAMPS® model (Hodur, 1997) has surface fluxes computed using a modified Louis scheme (Louis, 1982) as described by Wang *et al*. (2002). The domain configuration for the real-time atmospheric forecast includes three horizontally nested grids of 27 km, 9 km and 3 km and 30 vertical levels. The sea surface temperature (SST) used in forecasts was assimilated using satellite retrievals and ship observations. An example of COAMPS derived humidity fields compared against the rawinsondes data is shown in Fig. 7.

Another objective of CBLAST was to couple the mesoscale atmospheric model in COAMPS® with the Regional Ocean Modeling System (ROMS). ROMS is a high-resolution hydrodynamic model that has gained wide acceptance in the oceanographic community. ROMS was formulated for the region using detailed bathymetry. The model is forced by tides, outer shelf climatological inflows, observed downward radiative fluxes, and air-sea heat and momentum fluxes derived from the model SST and COAMPS forecast atmospheric conditions (Wilkin and Lanerolle, 2005).

The 3-dimensional evolution of regional ocean thermal stratification was simulated successfully, as validated by comparisons to mooring observations (Fig. 8) and satellite imagery (Wilkin, 2006). Tides proved important to the regional circulation, and accurate representation of

tidal variability in the model was achieved by assimilation of sea level data to adjust the tidal harmonic forcing open boundary conditions (He and Wilkin, 2006). One role for ROMS is to provide insight into process not resolved observationally. For example, lateral advection and sub-mesoscale mixing of heat are potentially significant in the local heat budget and ROMS was used to gauge the magnitude of horizontal heat transport compared to air-sea heat transfer (Wilkin, 2006).

COUPLED BOUNDARY LAYER PROCESSES. Marine scientists have long relied on flux-profile relationships that relate the turbulence fluxes of momentum, heat and moisture to their respective profiles of velocity, temperature, and water vapor. These relationships have been investigated during overland experiments since the mid-sixties that have generated a number of similar semi-empirical functions such as the commonly used form Businger-Dyer formulae (Businger, 1988). This approach is reasonably accurate as long as the boundary layer is horizontally homogeneous and the turbulent exchange is driven by a combination of mechanical and thermal forcing. However, the coastal boundary layers are often characterized by significant mesoscale variability in, e.g., surface temperature and roughness. Additionally, near the ocean surface, wave induced forcing is expected to influence the characteristics of the near surface flow.

Wave-induced effects have been shown to cause substantial departure from land-based parameterizations (e.g., Vickers and Mahrt, 1999; Smedman et al., 1999; and Hare et al. 1997) in the wave boundary layers (WBLs). The WBLs are defined in this overview as the region where the total momentum flux, even if assumed to be constant with height, has a significant wave-induced component (e.g., Hristov et al., 2003). Since land-based parameterizations are

formulated for turbulently driven processes (i.e., wind shear and buoyancy), they become increasingly inaccurate in the WBL as one nears the surface. This applies to both the atmospheric and ocean boundary layers. For example, coherent structures in the mixed layer, known as Langmuir circulations, are driven by wave-current interactions. These structures are believed to transport buoyancy and momentum and enhance the mixing. Additionally, intermittent turbulence and additional mixing is generated by wave-breaking. Neither of these processes is generally included in flux-profile relations, which implies that these processes are not accounted for in most models.

As a result, oceanographers and meteorologists often ignore wave-induced processes and treat the WBLs as a "black box." In most models, the fluxes of momentum and heat enter through the top of the box and then reappear unchanged at the bottom to drive the model as shown in Fig. 9. The details of wave-related processes that are actually responsible for the momentum and heat transport across the air-sea interface are generally ignored. In the sections that follow, we provide examples of ongoing investigations to determine and then parameterize the CBL processes that carry momentum and heat across the air-sea interface to improve numerical models.

Simulation Studies. Many of the investigations in CBLAST-LOW have relied on large eddy simulations (LES) and direct numerical simulations (DNS) to guide the observational process studies as summarized in Table 2. The numerical results provide a context for interpreting our measurements and investigating resolved processes, while our measurements have provided a means to evaluate sub-grid-scale parameterizations required by the models (Fig. 9). For example, in the process studies described below, LES is used guide investigations of wind-swell

interaction, wave-current interaction, and the impact of SST variability on the coupled boundary layers.

Momentum Exchange in Low Winds. The bulk aerodynamic formulae parameterize the sensible heat, latent heat, and momentum fluxes in terms of the more easily measured mean or bulk quantities using transfer coefficients. The transfer coefficient for momentum, i.e., the drag coefficient, computed from the CBLAST-LOW data set show good agreement in the mean with the TOGA COARE (TC) 3.0 algorithm (Fairall et al., 2003) as shown in Fig. 10. While there is some disagreement between the data and the parameterization at the highest wind speed (likely due to coastal/shoaling wave effects), the most significant disagreement is found at the lowest wind speeds.

Preliminary indications are that a number of physical processes driven by wind-wave interaction are responsible for this scatter. For example, for conditions with weak wind following faster moving swell, the wind stress may be reduced relative to the bulk prediction. These conditions are known as old seas and are commonly found over the ocean whenever waves, generated non-locally, propagate into a low wind region or whenever local seas slowly decay as a storm moves out of the region.

These investigations of wind-swell interaction have been guided by LES studies by Sullivan et al. (2004) that clearly show that fast moving swell in light winds can have a significant effect on the wind profile up to heights of O(10m). The LES indicate that this creates a wave-induced momentum flux divergence that accelerates the flow and a retarding pressure gradient, i.e., opposite to the momentum balance in classical boundary layers. Under these conditions, we

observe positive upward momentum flux and wave driven winds that produce a low-level jet (Fig. 11).

We have begun to investigate these processes using the ASIT data to examine the vertical structure of the turbulence in the surface layer, looking at how well the traditional predictions of the wind profiles compare with measurements over growing (young), fully developed (mature), and decaying (old) seas. As shown in Fig. 12, the bin-averaged profiles in unstable conditions all depart from their TC3.0 predictions as they approach the surface. The oldest wave show a velocity surplus while the youngest sea show a velocity deficit.

Direct Flux Measurements Beneath Surface Waves. The horizontal array of turbulence sensors on ASIT was used to directly measure heat and momentum fluxes. The oceanic momentum fluxes were estimated by direct covariance at 2.2 m depth and checked against an independent method that relied on the air-side measurements. The direct covariance estimates were made by integrating u'w' cospectra from zero up to an adaptive cutoff frequency below the wave band. This allowed estimation of the stresses carried in eddies approximately 1 m and larger. The independent estimates were made by assuming a slab-like mixed layer and interpolating between the measured wind stress at the surface and zero at the mixed layer base.

These estimates of stress match well at low wind speeds (Fig. 13), suggesting that all the stress at 2.2 m depth is carried in eddies larger than ~1 m. Stress being carried by large eddies is consistent with the predictions of Kaimal et al. (1972) for turbulence generated by shear and convective instabilities. It is also consistent with observed sizes of coherent structures known as Langmuir circulations (Plueddemann et al., 1996) discussed below.

At higher stresses, the ADV estimates fall slightly short of the expected estimates, suggesting that some stress was carried in smaller structures that we were unable to measure. One of our working hypotheses is that the smaller structures carrying the "missing" stress at fluxes larger than 0.06 Nm^{-2} may be the products of increased whitecapping or wave breaking under these higher stress conditions. These investigations are aided by a an acoustic device know as the BDCVP (see Table 1) that provides 1-cm resolution profiles of three component velocity vectors over a 1-m vertical span immediately below the water surface (Fig. 14).

Langmuir Circulation. A leading candidate for rapid heat and momentum transfer through the surface mixed layer is coherent circulation structures known as Langmuir circulation (LC). However, the fluxes associated with LC have never been measured, and attempts to parameterize LC mixing in 1-D ocean mixed-layer models are in their infancy.

The LES investigations of Li et al. (2005) guide our investigation of wave-current interactions associated with LC. These simulations have been conducted under a wide range of wind and wave conditions to investigate how the turbulence characteristics change with the sea state. For example, in fetch-limited conditions over shallow water, LES have shown that LC mixing is minimal and momentum exchange is dominated by shear driven turbulence. However, the LES have also shown that LC mixing strongly contributes to vertical exchange when waves propagate onshore from the open ocean.

Additional velocity sensors were deployed near ASIT to investigate LC mixing. Measurements of water velocity at the sea surface from the fanbeam ADCP show patterns of convergence and divergence at scales of a few tens of meters (Fig. 15), which can be used to identify Langmuir circulation (Plueddemann et al, 2001). When winds are moderate and waves

are small or decaying, LC is typically poorly developed as shown by the left panel in Fig. 15. However, the right panel shows that LC is clearly distinguishable under similar wind speeds when the wave field is growing. The observed strength of LC is strongly related to wind direction, emphasizing the role of limited fetch during Northerly winds south of Martha's Vineyard.

At low stresses, our initial studies have shown that shear, convection, and Langmuir circulations are all important mechanisms for generating stress-carrying turbulent eddies. At higher stresses it is likely that, in addition to these processes, wave breaking also plays a role in creating additional, smaller stress-carrying turbulent eddies. Our ultimate goal is to develop parameterizations of these processes for use in mixed layer models.

MESOSCALE MODULATION OF AIR-SEA EXCHANGE. Coordinated efforts during CBLAST-LOW were designed to observe and identify the processes that spatially modulate the vertical structure of the upper ocean that, in turn, can modulate the air-sea exchanges that couple the boundary layers over a wide range of horizontal scales.

Sea-Surface Temperature* (*SST) Variability. Sea surface temperature is a fundamental oceanic forcing of the atmosphere. In turn, the resulting changes in atmospheric stability impact the atmospheric forcing. SST during CBLAST-LOW had significant short-term temporal (e.g., diurnal) and small-scale (e.g., 5-10 km) spatial variability, which may have important impact on the atmosphere mesoscale forecast. An illustrative example of coupled boundary layer dynamics, as well as of the coordinated observations made during CBLAST, is provided in Fig. 16. The surface fluxes are clearly responding to the spatial variability in the SST field.

Dramatic change was seen in both latent and sensible heat fluxes (nearly 200 W/m^2 total) as the vessel moved across the narrow oceanic frontal zone. Snapshots like these over the course of the day show diurnal warming over the entire regions. The rate at which sub-regions warm and the corresponding response of the mixed layer will depend on the magnitude of the surface fluxes "locked" over these sub-regions.

Simulations of Spatial Variability. LES of SST variability was conducted to guide investigations of the effect of mesoscale SST variability on surface fluxes and the marine boundary layer structure (Skyllingstad et al. 2006). The basic scenario for the LES shown is to divide the simulation into regions of alternative warm/cold SST. Ambient air temperature upstream and downstream of the anomaly region are set equal to the SST values in Zone 1 and 4, respectively. This creates a neutrally stratified boundary layer upstream of the anomaly region. The boundary layer adjusts to neutral downstream from the anomaly region.

Simulations show that the spatial order, relative to the flow, of warm and cold anomalies has a direct impact on both the boundary-layer structure and the surface fluxes over this downstream region. When the warm anomaly is upstream from the cold anomaly, the downstream boundary layer exhibits a complex structure because of enhanced convective forcing and mixed layer deepening upstream from the cold anomaly. An internal boundary layer forms over the cold anomaly in this case, generating two distinct layers over the downstream region as shown in Fig. 17.

Similarities between the LES and the observations are evident. These results suggest that, for SST differences of 2-4 ^oC and mean wind speeds of 5-10 m s^{-1}, SST variability on scales of 5-20 km should be directly simulated in mesoscale models. Parameterization of surface fluxes and

boundary layer structure at these scales will be very difficult because of their dependence on sub-grid scale SST variability. However, simulations of similar flow over smaller scale fronts (< 5 km) indicate that small-scale SST variability might be represented in mesoscale models by relating the effective heat flux to the strength of SST variance.

Processes Responsible for SST Variability: Internal Waves. During conditions of low winds and strong insolation, quasi-periodic banded structures were observed at scales of *O*(50-2000 m) in infrared SST measured from the *FV Nobska* and Cessna Skymaster. Previous observations made in similar conditions have suggested that these organized structures are associated with internal (oceanic gravity) waves (*Walsh et al.*, 1998; *Marmorino et al.*, 2004), but those prior studies lacked the coincident subsurface measurements necessary to unambiguously identify the mechanisms responsible for the surface signature. *Walsh, et al.* 1998 argued that the oceanic internal waves produced a signature in SST by modulating the vertical mixing in the diurnal warm layer, whereas *Marmorino, et al.* argued that internal wave vertical straining modifies the magnitude of the cool skin effect due to evaporative cooling. The aircraft, ship, and mooring data allow evaluation of both hypotheses as described by *Farrar et al.* (2006)

Processes Responsible for SST Variability: Coherent Structures. Additional small-scale structures within the IR imagery suggest mechanisms that drive or enhance exchange under low winds have been observed by Zappa and Jessup (2005). In particular, extensive regions (*O*(1 km)) are observed with embedded sharp coherent temperature ramps of *O*(0.5ºC) with spacing of *O*(10 m) during light to moderate winds (2.5 to 5 ms^{-1}) as shown in Fig. 18. The lack of coherent parallel features in the visible imagery suggests that the ocean surface features observed in the IR

imagery are not related to surface gravity waves (Jessup, 1996). Instead, preliminary analysis suggests that these coherent ramp-like structures are IR signatures of "billows" due to shear instabilities.

For wind speeds greater than 5 ms^{-1}, there was significantly less spatial variability in SST, but distinct row/streak structures were observed aligned with the wind and perpendicular to the waves. Combined with a well-mixed layer, the conditions provide a highly favorable environment for the development of LC. The horizontal spacing of these features coincided with wind-aligned surface slicks and bubbles visible in the video and agrees well with the scale expected for Langmuir cells. These fine-scale measurements demonstrate processes that directly affect the thermal boundary layer and therefore are important to upper-ocean mixing and transport dynamics as well as the magnitude and distribution of air-sea fluxes.

COUPLED FORECASTING AND FOG FORMATION. As with terrestrial boundary layers, our understanding and ability to simulate processes in stratified (stable) marine ABLs lags our understanding of convective ABL processes. Over the past several decades, marine investigations have concentrated on neutral to slightly convective MABLs and our parameterizations have been tuned to these conditions (e.g., Edson et al., 2004). In contrast, oceanographers have focused on neutral to stratified boundary layer and the inherent complexity that arises due to patchy and intermittent turbulence.

The ABL over the CBLAST region was typically stable during the first half of the summer due to the combination of advection and a slowly warming coastal ocean (Crofoot 2004). This is a common occurrence along the East coast during the late spring and early summer. Stable marine ABL is also a common occurrence on the West coast, particularly when northerly winds

drive coastal upwelling. As residents of both coasts can attest, these stable MABLs are often characterized by fog and cool summertime weather.

Our initial investigations have shown significant differences between direct covariance and bulk fluxes in stable conditions, particularly when the moisture flux is directed downward (Fig. 19). These periods of downward moisture flux are often associated with foggy conditions as shown in Fig. 20. These inaccurate parameterizations present an obvious obstacle to accurate forecasts of fog. Therefore, improvement of heat flux parameterizations in stable conditions is a main objective of ongoing investigations.

COAMPS analysis has shown that improved parameterizations are only part of improvements required for accurate forecasts of fog. For example, COAMPS runs have shown that its ability to predict fog is extremely sensitive to the SST used in the model. These sensitivity tests indicate that a 4^{o}C increase in SST forces the model prediction to go from heavy fog to no fog as shown in Fig. 21. SST variability of several degrees is the rule rather than the exception in coastal regions where, as shown by ROMS, upwelling and lateral advection often dominate the dynamics.

One solution to combat this sensitivity is accurate SST estimate from remote sensing. However, weather systems often obscure the surface with clouds and fog that is impenetrable to IR remote sensing. New technologies are starting to be capable to peer through clouds and fog, but these suffer from low resolution and biases. Therefore, a reasonable solution to this problem is a truly coupled atmosphere-ocean forecast system that provides the necessary spatial and temporal resolution, complemented with improved estimates of SST from remote and in situ observing systems. CBLAST investigations continue with this goal in mind.

SUMMARY An unprecedented data set was collected on both sides of the ocean-atmosphere interface during the CBLAST-LOW experiments. This included the first direct measurements of heat and momentum exchange on both sides of the air-sea interface. These measurements are being used to investigate the processes that govern the exchange of momentum, heat, and mass across the coupled boundary layers. These processes studies have involved close collaboration with numerical modelers and many of these investigations are driven by the numerical simulations summarized in Table 2. Our initial investigations has shown that ocean waves have a significant impact on air-sea exchange and coupled boundary layer processes even under light wind conditions. These studies have also shown that mesoscale and finer scale variability in the sea surface temperature field strongly modulates the vertical structure of the coupled boundary layers. Continued investigations are expected to improve the predictive capabilities of a coupled air-sea models. An extended version of this article and additional information about the CBLAST program can be found at http://www.whoi.edu/science/AOPE/dept/CBLAST/low/cblastlow.html.

**In Memoriam:* This research is dedicated and in tribute to Dr. Timothy Crawford (1948-2002). Tim always stated "It's not about the flying. It's about the science." That was one of the favorite quotes from the late Dr. Timothy L. Crawford, Director of the Field Research Division (FRD) of the National Oceanic and Atmospheric Administration's (NOAA) Air Resources Laboratory (ARL). The scientific community suffered a tragic loss with the passing of Dr. Timothy L. Crawford on August 3, 2002. He was 53 years old.

Acknowledgements: This work was supported by the Office of Navel Research.

REFERENCES

Austin, T., J. Edson, W. McGillis, M. Purcell, R. Petitt, M. McElroy, J. Ware, C. Grant, and S Hurst, 2002: A network-based telemetry architecture developed for the Martha's Vineyard coastal observatory. *IEEE J. Oceanic Eng.*, **27**, 228-234.

Businger, J. A., 1988: A note on the Businger-Dyer profiles. *Bound.-Layer Meteorol*., **42**, 145-151.

Crofoot, R. F., 2004: Investigations of scalar transfer coefficients in fog during the Coupled Boundary Layers and Air-Sea Transfer experiment: A case study, *M.S. Thesis*, WHOI/MIT Joint Program.

Edson, J. B., C. J. Zappa, J. A. Ware, W. R. McGillis, and J. E. Hare, 2004: Scalar flux profile relationships over the open ocean. *J. Geophys. Res.*, **109**, C08S09, doi:10.1029/2003JC001960.

Fairall, C. W., E. F. Bradley, J. E. Hare, A. A. Grachev, J. B. Edson, 2003: Bulk parameterization of air–sea fluxes: Updates and verification for the COARE algorithm, *J. Climate*, **16**, 571–591.

Farrar, J.T., R.A. Weller, C.J. Zappa, and A.T. Jessup, 2006: Subsurface expressions of sea surface temperature variability under low winds, in preparation

Grimmett, T. K., J. R. Grench, and G. H. Crescenti, 2006: Spatial variability of CD over water in light winds measured from an instrumented aircraft. *Bound.-Layer. Meteor.*, submitted.

Hare, J.E., T. Hara, J.B. Edson, and J.M. Wilczak, 1997: A similarity analysis of the structure of air flow over surface waves. *J. Phys. Oceanogr.*, **27**, 1018-1037.

He, R. and J. Wilkin, 2006: Tides on the Southeast New England Shelf: A View from a Hybrid Data Assimilative Modeling Approach, *J. Geophys. Res.*, submitted.

Hodur, R.M., 1997: The Naval Research Laboratory's Coupled Ocean/Atmosphere Mesoscale Prediction System (COAMPS). *Mon. Wea. Rev.*, **125** 1414-1430.

Hristov, T. S., S. D. Miller, and C. A. Friehe, 2003: Dynamical coupling of wind and ocean waves through wave-induced air flow. *Nature*, **422**, 55-58.

Kaimal, J.C., J.C. Wyngaard, Y. Izumi, and O.R. Coté, 1972: Spectral characteristics of surface-layer turbulence. *Quart. J. Roy. Meteor. Soc.*, **98**, 563-589.

Kraus, E.B. and J.S. Turner, 1967: A one-dimensional model of the seasonal thermocline. II. The general theory and its consequences. *Tellus*, **19**, 98-105.

Large, W. G., J. C. McWilliams, and S. C. Doney, 1994: Ocean vertical mixing: A review and a model with a nonlocal k-profile boundary layer parameterization. *Rev. Geophys.*, **32**, 363-403.

Li, M., C. Garrett and E. Skyllingstad. 2005: A regime diagram for classifying turbulent large eddies in the upper ocean. *Deep-Sea Res. I*, **52**, 259-278.

Louis, J. F., 1979: A parametric model of vertical eddy fluxes in the atmosphere. *Bound.-Layer. Meteor.*, **17**, 187-202.

Marmorino, G.O., G.B. Smith, and G.J. Lindemann, 2004: Infrared imagery of ocean internal waves, *Geophys. Res. Lett.*, **31**, L11309, doi:10.129/2004GL020152.

Mellor, G. L., and Yamada, T., 1982: Development of a closure model of geophysical flows, *Rev. Geophys. Space Physics*, **20**, 851-875.

Plueddemann, A.J., J.A. Smith, D.M. Farmer, R.A. Weller, W.R. Crawford, R. Pinkel, S. Vagle and A. Gnanadesikan, 1996: Structure and variability of Langmuir circulation during the Surface Wave Processes Program. *J. Geophys. Res.*, **101** (C2), 3525-3543.

Plueddemann, A.J., E.A. Terray and R. Merewether, 2001: Design and performance of a self-contained, fan-beam ADCP. *IEEE J. Oceanic Eng*., **26**(2), 252-258.

Price, J., R. Weller and R. Pinkel, 1986: Diurnal Cycling: Observations and Models of Upper Ocean Response to Diurnal Heating, Cooling and Wind Mixing., *J. Geophys. Res.*, **91**, 8411-8427.

Pritchard, M. and R.A. Weller, 2005. Observations of internal bores and waves of elevation on the New England inner continental shelf during summer 2001. *J. Geophys. Res.*, **110**, C03020, doi:10.1029/2004JC002377.

Smedman, A., U. Högström, H. Bergström, A. Rutgersson, K. K. Kahma, and H. Pettersson, 1999: A case study of air-sea interaction during swell conditions. *J. Geophys. Res.*, **104**, 25833-25851.

Skyllingstad, E. D., D. Vickers, L. Mahrt, and R. Samelson, 2006: Effects of mesoscale sea-surface fronts on the marine boundary layer. *Boundary-Layer Meteor*., submitted.

Sullivan, P. P., et al., 2004: Large-eddy simulations and observations of wave-driven boundary layers, *Proc. 16th Symp. on Boundary Layers and Turbulence*, Portland, ME, Amer. Meteor. Soc., This Volume.

Vickers, D. and L. Mahrt, 1999: Observations of non-dimensional wind shear in the coastal zone, *Quart. J. Roy. Met. Soc.*, *125*, 2685-2702.

Vickers, D., and L. Mahrt (2005), A solution for flux contamination by mesoscale motions with very weak turbulence, *Bound.-Layer. Meteor.*, in press.

Vickers, D., and L. Mahrt, 2005: Aircraft observations of air-sea fluxes: Bulk modeling and sea-surface temperature variability. *Bound.-Layer. Meteor.*, submitted.

Walsh, E.J., R. Pinkel, D. E. Hagan, R. A. Weller, C. W. Fairall, D. P. Rogers, S. P. burns, and M. Baumgartner, 1998: Coupling of internal waves on the main thermocline to the diurnal surface layer and sea surface temperature during the Tropical Ocean-Global Atmosphere Coupled Ocean-Atmosphere Response Experiment. *Journal of Geophysical Research,* **103**, 12613-12628.

Wang, S., Q. Wang, and J. Doyle, 2002; Some improvement of Louis surface flux parameterization. *15th Symposium on Boundary layers and Turbulence*, American Meteorological Society, 15-19, July 2002, Wageningen, the Nettherland. 547-550.

Wilkin, J., 2006: Modeling the summertime heat budget of southeast New England shelf waters. *J. Phys. Oceanogr*, submitted.

Wilkin, J., and L. Lanerolle, 2005: Ocean Forecast and Analysis Models for Coastal Observatories, in *Ocean Weather Forecasting: An Integrated View of Oceanography,* E. Chassignet and J. Verron, Eds., pp. 549-572, Springer.

Zappa, C.J., and A.T. Jessup, 2005: High resolution airborne infrared measurements of ocean skin temperature, *Geoscience and Remote Sensing Letters*, ***2*** (2), doi:10.1109/LGRS.2004.841629.

Table 1. Instrumentation deployed on and around ASIT during the 2003 IOP.		
Sensors	Variables	Nominal Measurement height(s)
Pyrgeometer	IR radiative flux	22 m
Pyranometer	Solar radiative flux	22 m
Rain Gauge	Precipitation	13 m
Sonic Anemometer	Fast response 3-component velocity, temperature	20, 18, 15 m
Pressure sensor	Mean pressure.	6.5, 9, 10, 18 m
T/RH sensor	Mean temperature, relative humidity	5, 7, 9, 13.5, 18, 21 m
Sonic anemometer, infrared hygrometer static pressure sensor	Fast response 3-component velocity, temperature, water vapor, static pressure	4, 6.5, 10 m
Static pressure sensor	Fast response static pressure	6.5, 10m
Profiling package: T/RH sensor, sonic anemometer	Mean Temperature, relative humidity, horizontal velocity	2.5 to 16 m
Radiometer	Sea surface temperature	0 m
Laser altimeter, microwave altimeter	Surface elevation, wave height	0 m
Microwave altimeter	Surface elevation, wave height	0 m
Fanbeam ADCP	2-D maps of surface velocities	0 m
Bistatic Coherent Doppler Velocity Profiler (BCDVP)	3-component velocity profiles	-1 to 0 m
High resolution acoustic Doppler current profiler (ADCP)	Current profiles	-3.5 to 0 m
Acoustic Doppler velocimeter (ADV), thermistor, pressure sensor	Fast response 3-component velocity, temperature, wave height and direction	-3.5 m
Conductively, temperature, depth (CTD) sensor	Salinity, temperature, depth	-1.5, -5, -12 m
Broadband Acoustic Doppler Current Profiler (BADCP)	Current profiles, vertical velocity profile	-13 to -0.5 m
Acoustic Doppler current profiler (ADCP)	Current profiles	-13 to -0.5 m
Current meters	Fast response 3-component velocity	-12 m

Table 2. Simulations Studies Conducted in Support of CBLAST.		
Study	Simulation	PI(s)
Turbulence airflow over swell and its impact on wave boundary layer structure.	Atmospheric LES with BC conditions imposed by resolved waves (swell) and parameterized surface roughness.	P. Sullivan, J. Edson, J. McWilliams, T. Hristov
Simulations of atmospheric boundary layer in CBLAST region.	Atmospheric LES using boundary conditions from COAMPS mesoscale model	P. Sullivan, S. Wang
Simulation of atmospheric boundary layer evolution over mesoscale SST fronts.	Atmospheric LES over step changes in sea surface temperature.	E. Skyllingstad, L. Mahrt, D. Vickers
Detailed studies of the coupling mechanisms between the air and water turbulent flows.	DNS using fully-nonlinear free-surface coupled boundary conditions	D.K.P. Yue, L. Shen
Simulations of the effect of wave breaking on the ocean surface layer	Oceanic DNS with stochastic wave breaking.	P. Sullivan, J. McWilliams, K. Melville
Impacts of breaking waves and Langmuir circulation on the ocean mixed layer	Ocean LES with Craik-Leibovich vortex force and intermittent stress transmission from a spectrum of breaking wave events	P. Sullivan, J. McWilliams, K. Melville
Deepening of the ocean mixed layer by Langmuir and shear turbulence	Stratified ocean LES with Craik-Leibovich vortex force and constant surface stress	M. Li, A. Plueddemann

FIGURE CAPTION LIST

Figure 1. A few of the physical processes governing air-sea exchange across the coupled boundary layers.

Figure 2. A diagram of the CBLAST region showing the location of the surface moorings, ASIT, subsurface moorings, and MVCO sensors deployed during the IOP in the summer 2003.

Figure 3. A schematic representation of the MVCO showing the location of the meteorological mast, seanode, and ASIT. The cutout shows the actual location of these elements on the South shore of Martha's Vineyard.

Figure 4. a) Experiment setup for the ASIT during CBLAST. The photo indicates the location of the fixed array, profiler and subsurface array (beneath surface). **b)** The subsurface horizontal array photographed from ASIT. The booms support fast response velocity and temperature sensors.

Figure 5. a) Instrumentation deployed on the Nobska during the 2003 IOP. Bow instrumentation included a direct covariance flux system and IR radiometers. The boom supported an array of temperature/salinity sensors for high-resolution vertical profiles. b) Photo taken from the Air-Sea Interaction Tower at MVCO of the SCIMS catamaran accompanied by R/V Asterias during a southeasterly survey transect on August 15, 2003. Numerous banded surface film features (light areas) evident in the field of view were quantified by SCIMS instrumentation.

Figure 6. An illustrative example of the SST maps provide by the IR system. These preliminary images were provided to CBLAST-LOW PI after each run to assist in coordinated ship and aircraft observations.

Figure 7. Temporal evolution of specific humidity vertical profiles from Nantucket rawinsonde (top panel), and COAMPS 3-km grid forecast (bottom panel). The red (*) at the bottom indicate the time of all soundings used to generate the plot.

Figure 8 Time series of vertical temperature profile at Mooring-F. Upper panel is modeled, lower panel is measured.

Figure 9. A schematic showing how simulations are being used to improve the mesoscale model parameterizations in concert with the observational process studies. The black box represents the processes shown in gray that are generally not included in flux parameterizations. CBLAST investigations are aimed at including these subgrid-scale processes in improved parameterizations of the coupled boundary layers.

Figure 10. Individual and bin-averaged drag coefficient estimates. The black line is the TC3.0 parameterization.

Figure 11. Profiles of horizontal velocity components normalized by their geostrophic values from LES over a variety of surfaces. The blue, red and magenta profiles simulate conditions over swell.

Figure 12. The left panel shows results from two of the LES runs for winds over swell in unstable and neutral conditions. The right panel shows measured (symbols) and MO predicted (lines) velocity profiles average over 3 wave age classes denoting young, mature, and old seas.

Figure 13. Comparison of subsurface stress estimates from direct covariance measurements (ADV) and a simple mixed-layer model (expected). The red dots indicate bin-averaged results. The vertical line demarcates stresses measured at wind speeds above (to the right) and below (to the left) 7 ms^{-1}.

Figure 14. A 100 second profile timeseries of a.) surface elevation, b.) acoustic backscatter levels, c.) low pass filtered vertical velocity and d.) u'w' stress component correlations measured under short period, limited fetch wind waves. Bubbles injected during a wave breaking event at t=7 seconds were entrained by a sub-surface circulation cell seen in the vertical velocity profiles that have the wave-period motions filtered out. The results have been mapped into a surface-following coordinate system

Figure 15. Time-range plots of water velocity at the sea surface based on fanbeam ADCP measurements during CBLAST-LOW. The wind speed was approximately the same during the two periods shown. However, the waves were fetch-limited and smaller in the left panel and from the open ocean and larger in the right panel.

Figure 16. On the left, subsurface thermal structure (lower), sensible and latent surface heat fluxes (middle), and atmospheric temperature from the Pelican aircraft (upper) associated with the ship track shown on the right executed by the *FV Nobska* on the afternoon of August 19, 2003. The response of the atmospheric boundary layer to the SST field is evident, but the strong spatial variation of heat fluxes also affects the subsequent evolution of the SST field.

Figure 17. Cross section plots in the vertical and horizontal direction showing (a) horizontal velocity (m s^{-1}), and (b) potential temperature (^{o}C). Surface temperatures are 18 ^{o}C in Zone 1, 16 ^{o}C in Zone 2, 20 ^{o}C in Zone 3, and 18 ^{o}C in Zone 4, and the wind is from the left. The simulations indicate that the response of the atmospheric boundary layer to these small-scale SST variations would be difficult to parameterize because the boundary layer response depends on whether flow is from warm to cold water or vice-versa.

Figure 18. Left: IR image showing coherent ramp structures observed on August 14, 2003 in the afternoon. The wind speed (Blue Arrow) is roughly 4 m s^{-1} from the West and the surface

current (Green Arrow) is 17 cm s^{-1} from the East. The dominant spatial scale of the variability in temperature across these coherent ramps is 14.7 m, and they extend over several km. The fact that upper-ocean thermal stratification was breaking down at this time and that the features are roughly perpendicular to the surface current suggests that these ramp-like structures may be associated with shear instabilities. Right: IR image depicting Langmuir circulation observed on August 25, 2003 in the morning. The wind speed (Blue Arrow) is roughly 5 m s^{-1} and the surface current (Green Arrow) is 47 cm s^{-1}, both from the West-Southwest. The dominant scale between these cool bands is 21.0 m, and their orientation relative to the wind and wave directions suggests that these features are associated with Langmuir circulation.

Figure 19. Comparison of direct covariance versus bulk aerodynamic latent heat fluxes measured from ASIT.

Figure 20. Time series of the latent heat fluxes and visual evidence for the presence of fog during periods of downward moisture flux.

Figure 21. The sensitivity of fog formation to SST as indicted by model prediction of liquid water content.

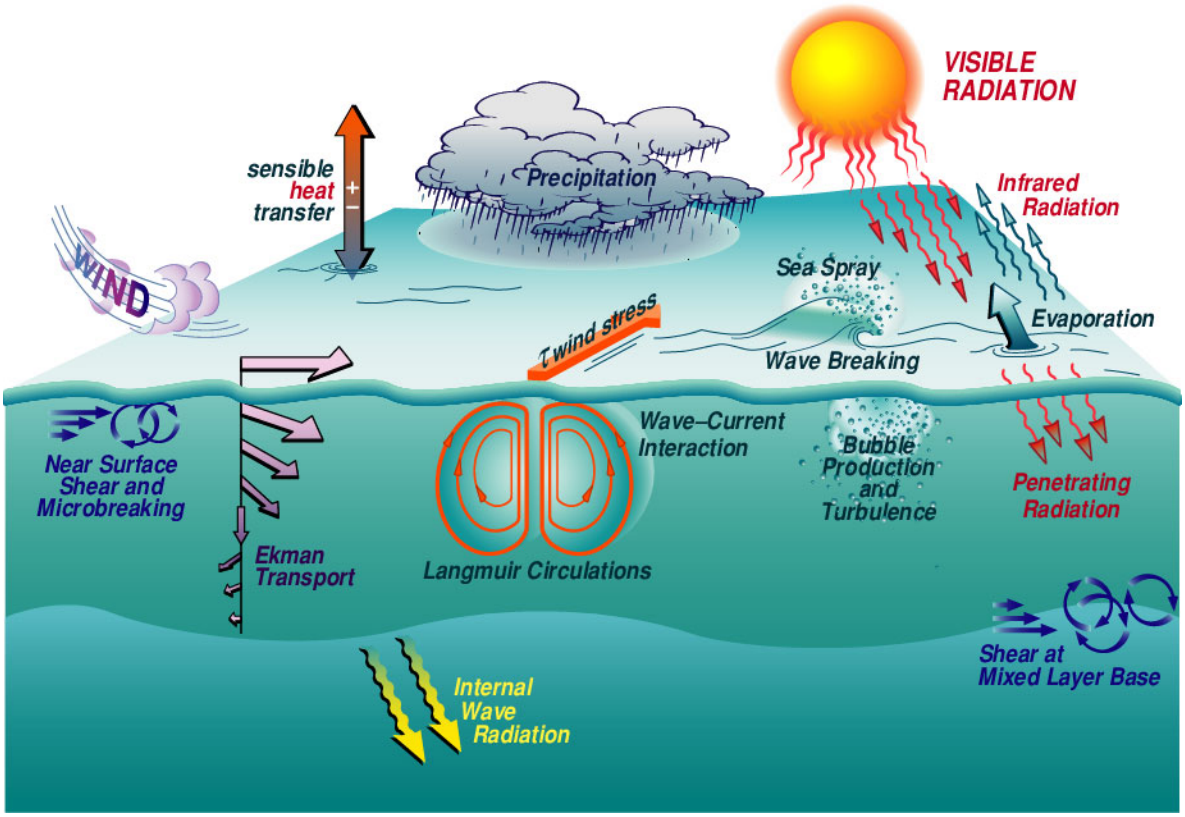

Figure 1. A few of the physical processes governing air-sea exchange across the coupled boundary layers.

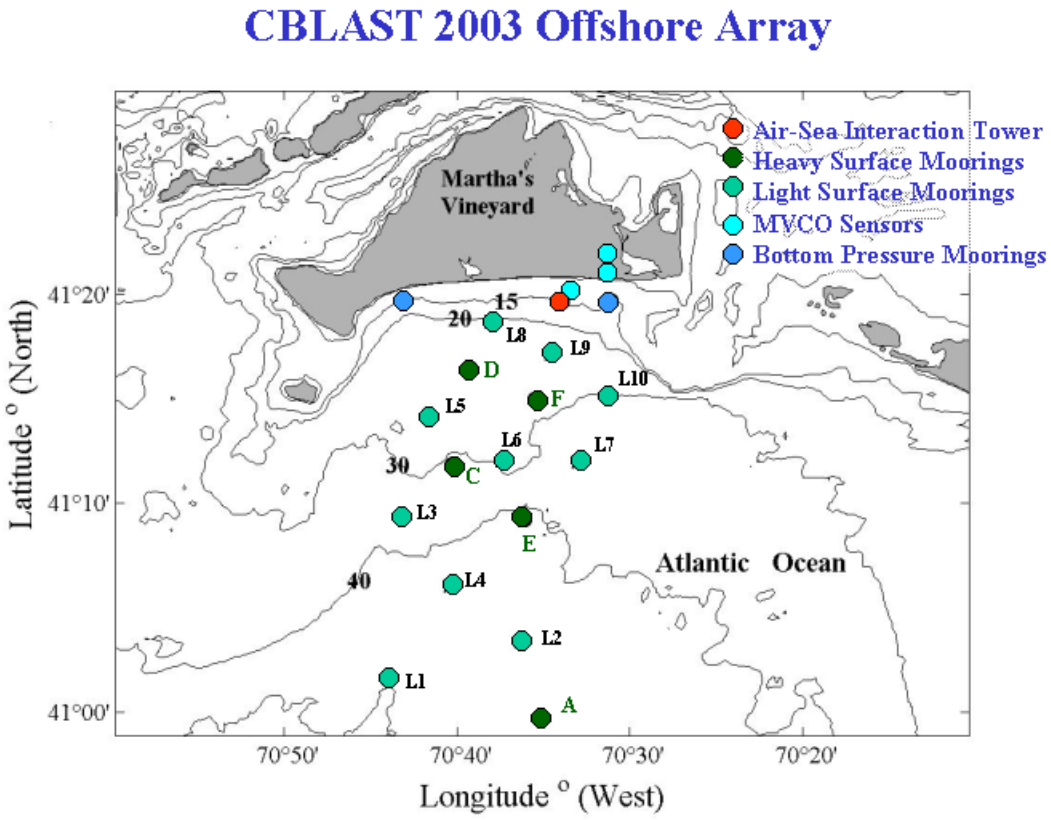

Figure 2. A diagram of the CBLAST region showing the location of the surface moorings, ASIT, subsurface moorings, and MVCO sensors deployed during the IOP in the summer 2003.

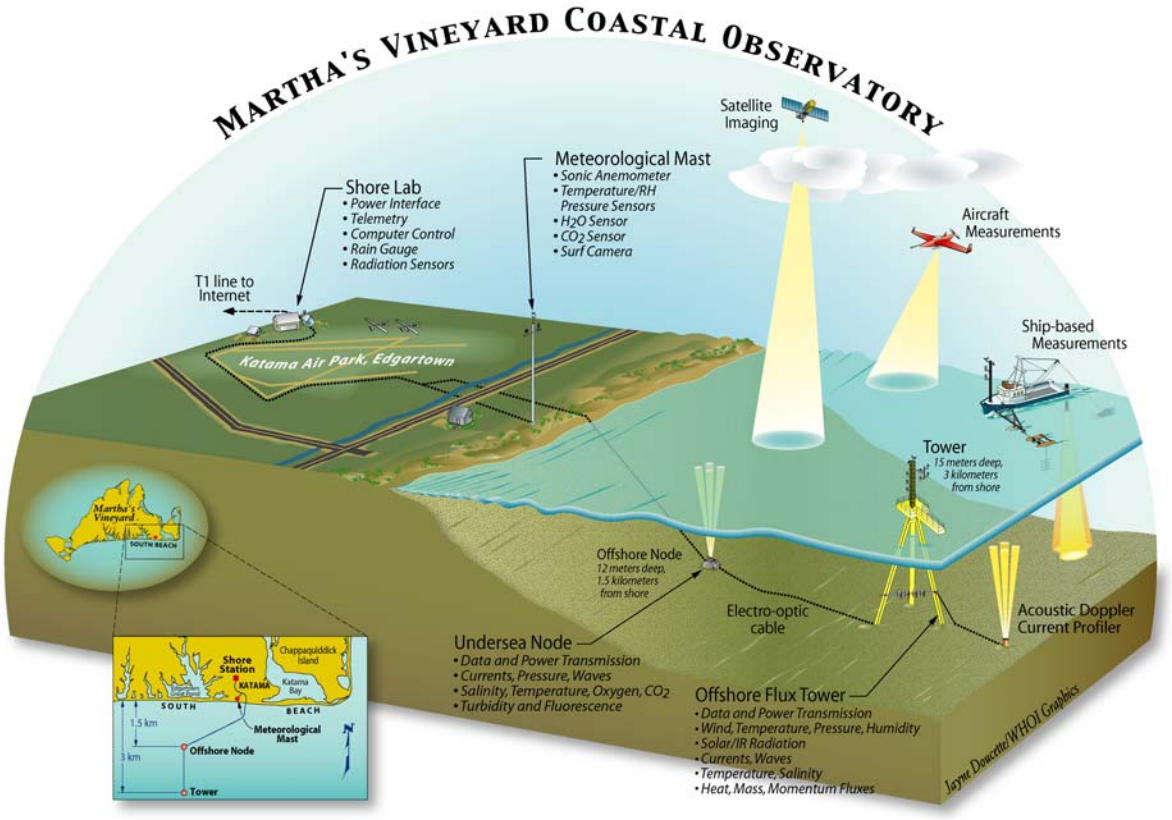

Figure 3. A schematic representation of the MVCO showing the location of the meteorological mast, seanode, and ASIT. The cutout shows the actual location of these elements on the South shore of Martha's Vineyard.

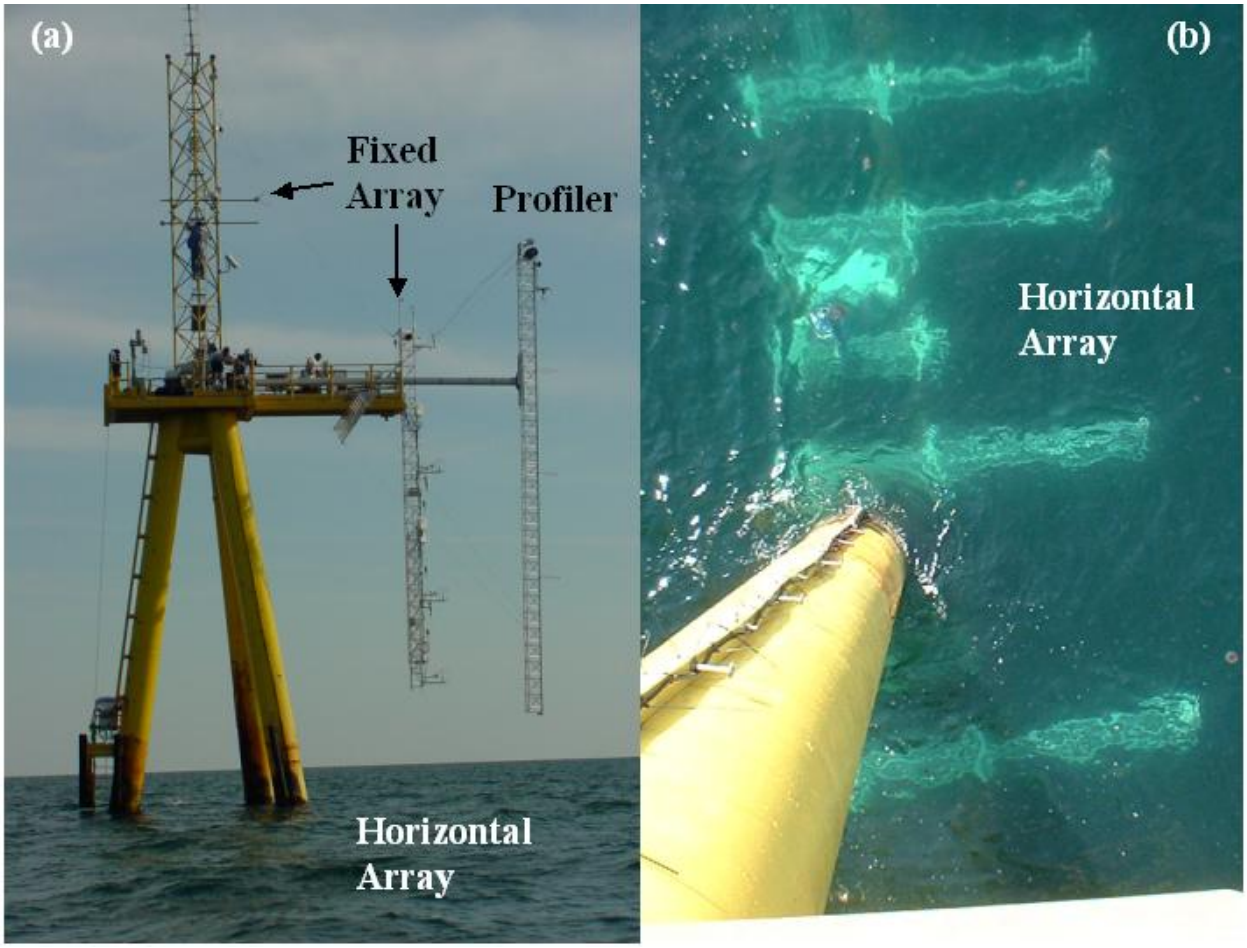

Figure 4. a) Experiment setup for the ASIT during CBLAST. The photo indicates the location of the fixed array, profiler and subsurface array (beneath surface). **b)** The subsurface horizontal array photographed from ASIT. The booms support fast response velocity and temperature sensors.

Figure 5. a) Instrumentation deployed on the Nobska during the 2003 IOP. Bow instrumentation included a direct covariance flux system and IR radiometers. The boom supported an array of temperature/salinity sensors for high-resolution vertical profiles. b) Photo taken from the Air-Sea Interaction Tower at MVCO of the SCIMS catamaran accompanied by R/V Asterias during a southeasterly survey transect on August 15, 2003. Numerous banded surface film features (light areas) evident in the field of view were quantified by SCIMS instrumentation.

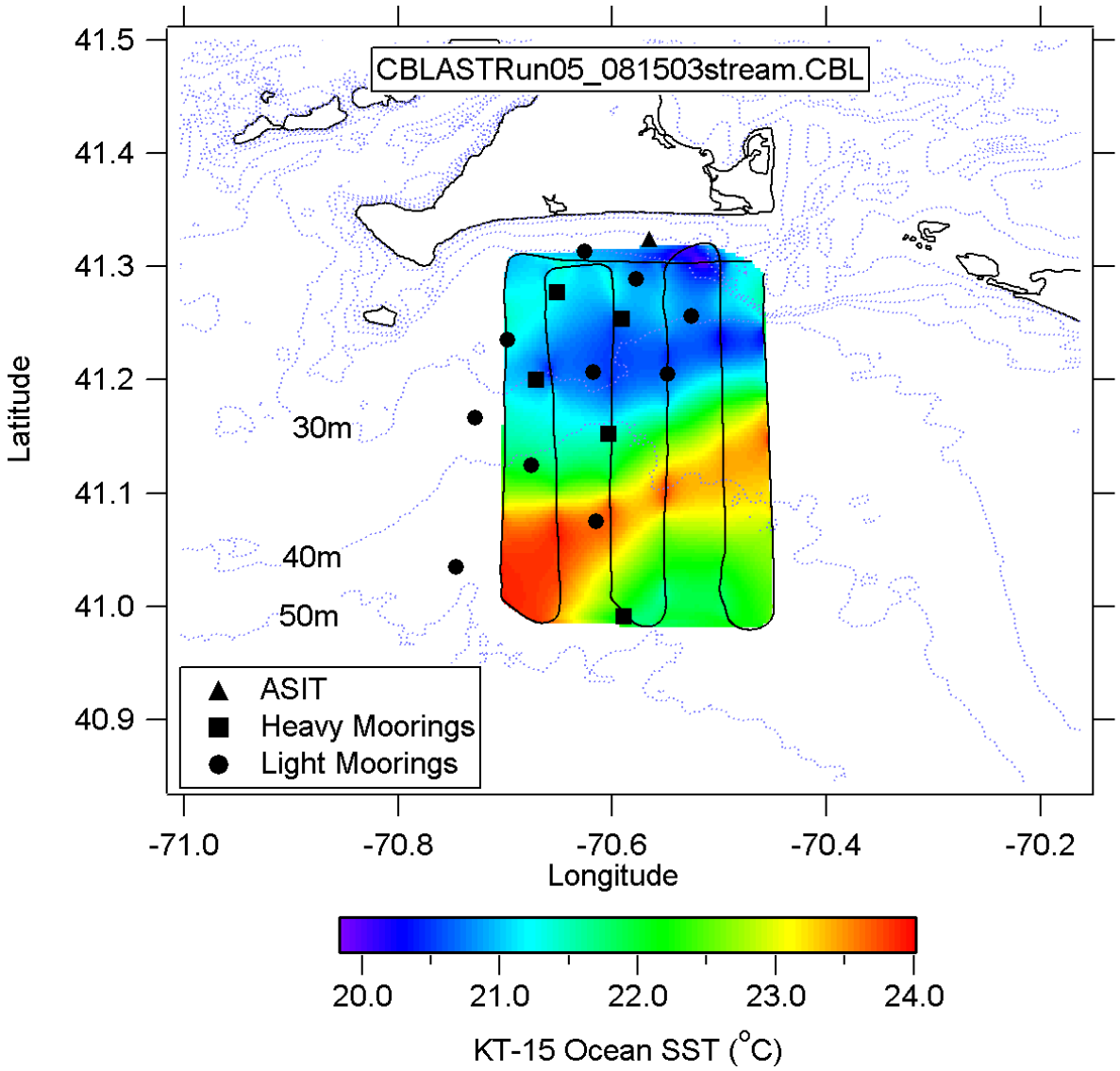

Figure 6. An illustrative example of the SST maps provide by the IR system. These preliminary images were provided to CBLAST-LOW PI after each run to assist in coordinated ship and aircraft observations.

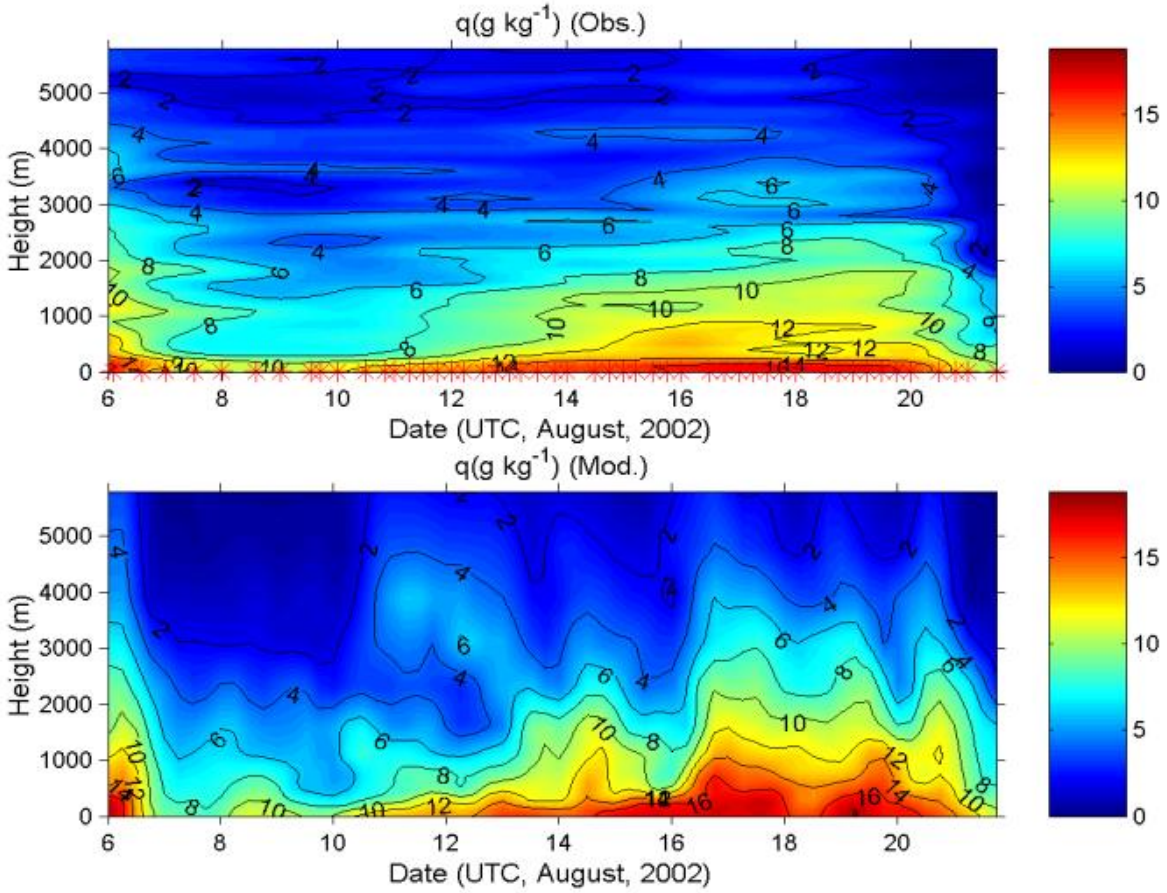

Figure 7. Temporal evolution of specific humidity vertical profiles from Nantucket rawinsonde (top panel), and COAMPS 3-km grid forecast (bottom panel). The red (*) at the bottom indicate the time of all soundings used to generate the plot.

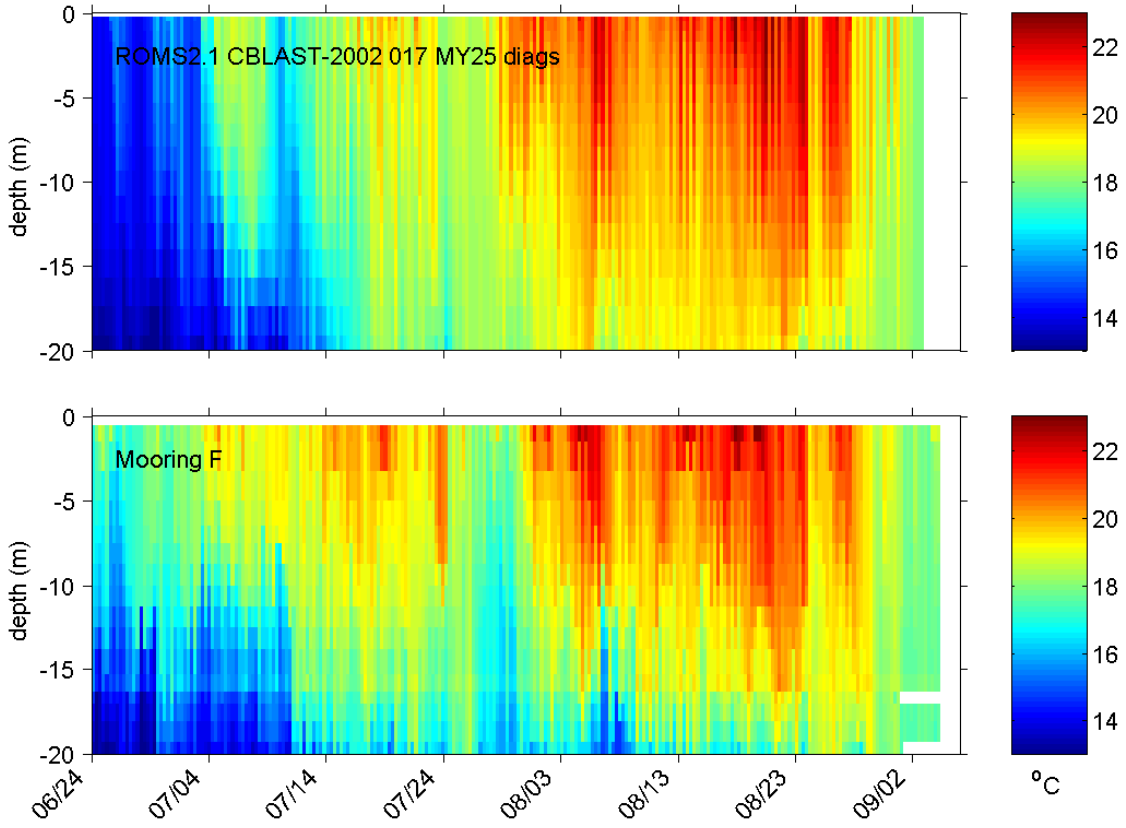

Figure 8. Time series of vertical temperature profile at Mooring-F. Upper panel is modeled, lower panel is measured.

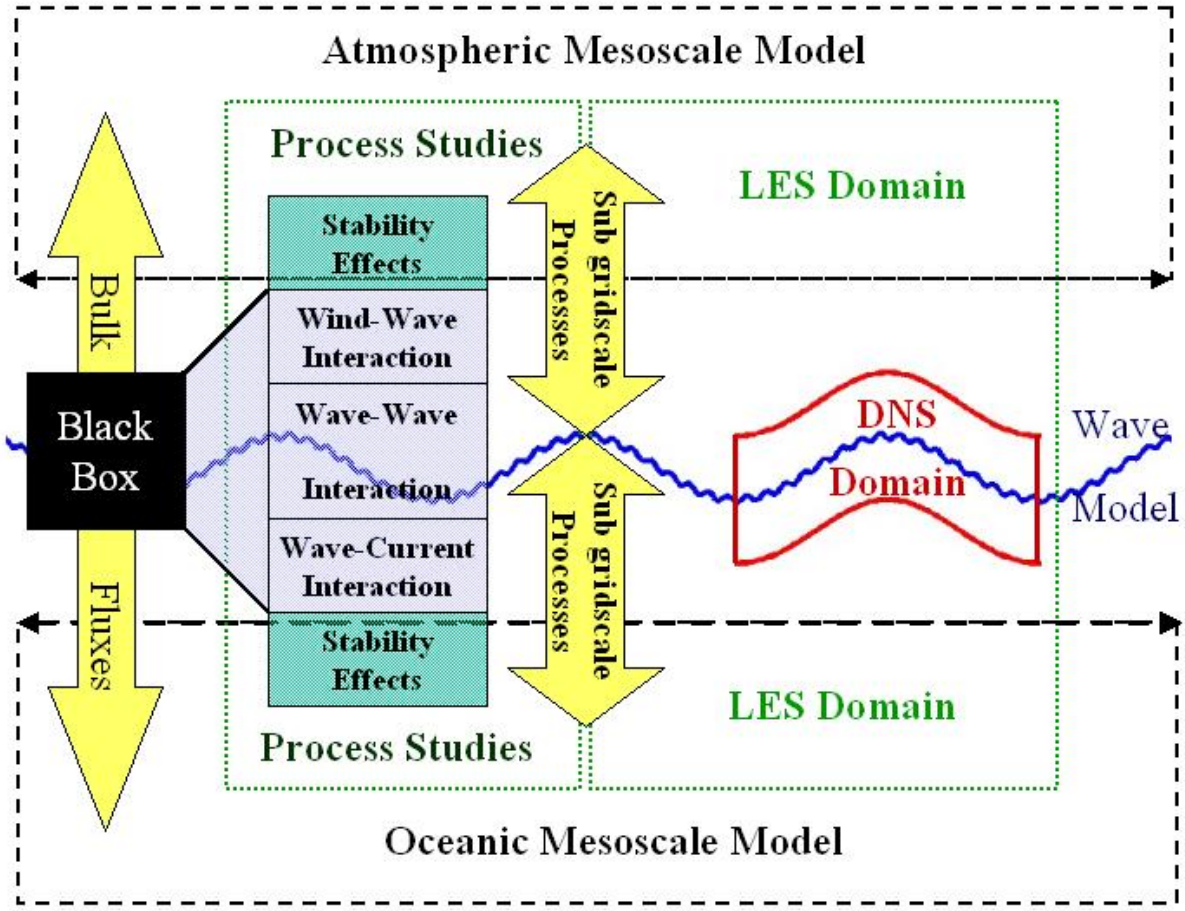

Figure 9. A schematic showing how simulations are being used to improve the mesoscale model parameterizations in concert with the observational process studies. The black box represents the processes shown in gray that are generally not included in flux parameterizations. CBLAST investigations are aimed at including these subgrid-scale processes in improved parameterizations of the coupled boundary layers.

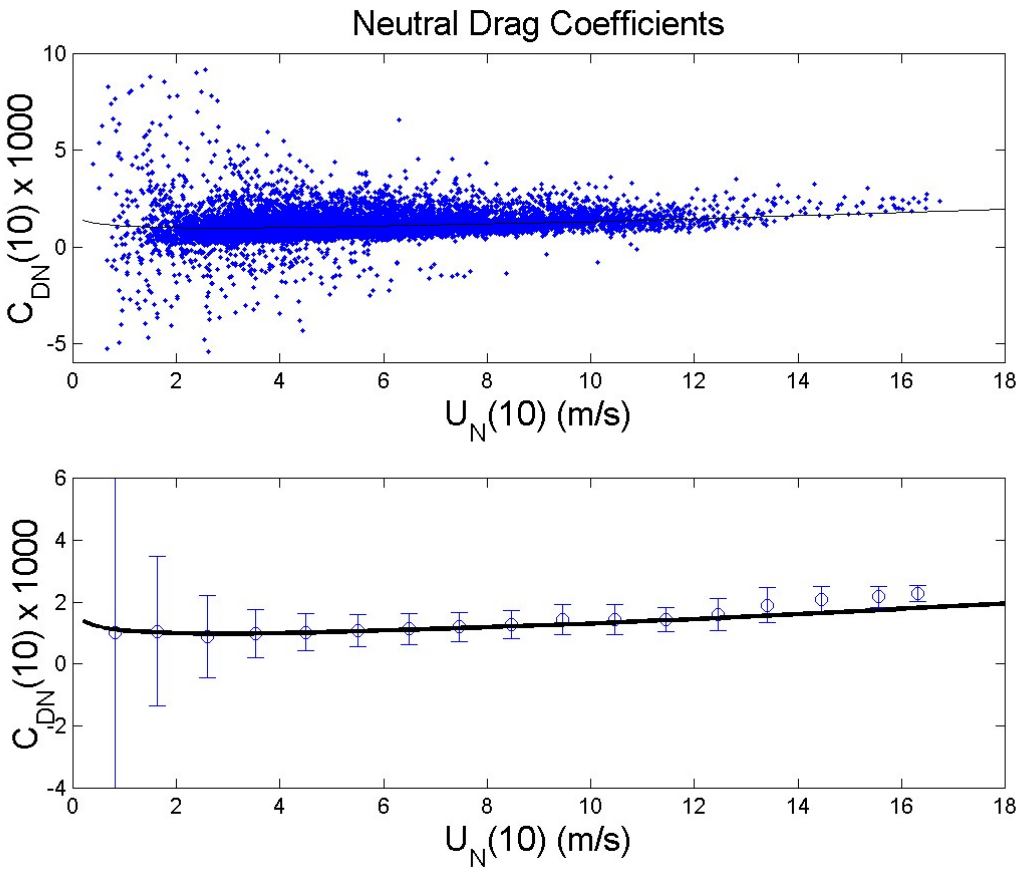

Figure 10. Individual and bin-averaged drag coefficient estimates. The black line is the TC3.0 parameterization.

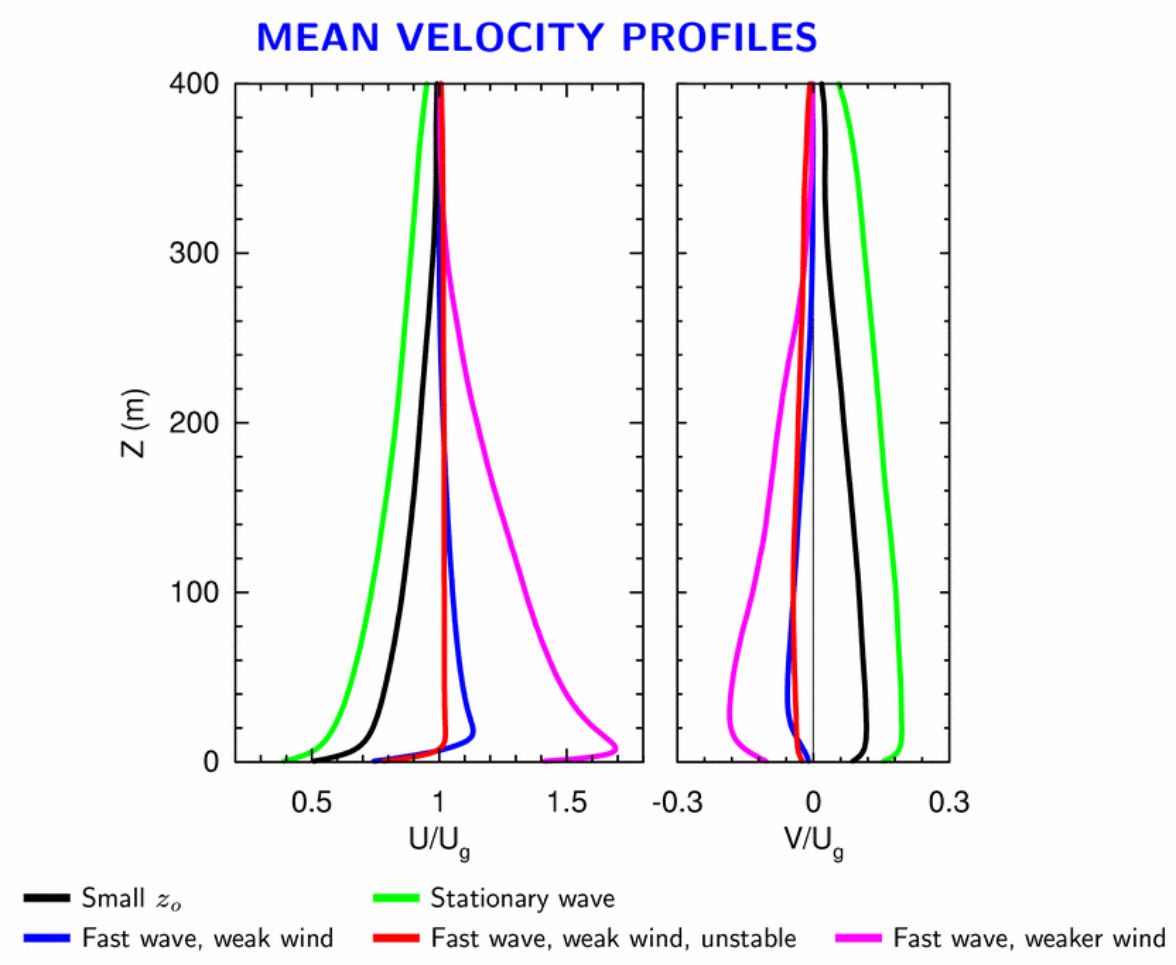

Figure 11. Profiles of horizontal velocity components normalized by their geostrophic values from LES over a variety of surfaces. The blue, red and magenta profiles simulate conditions over swell.

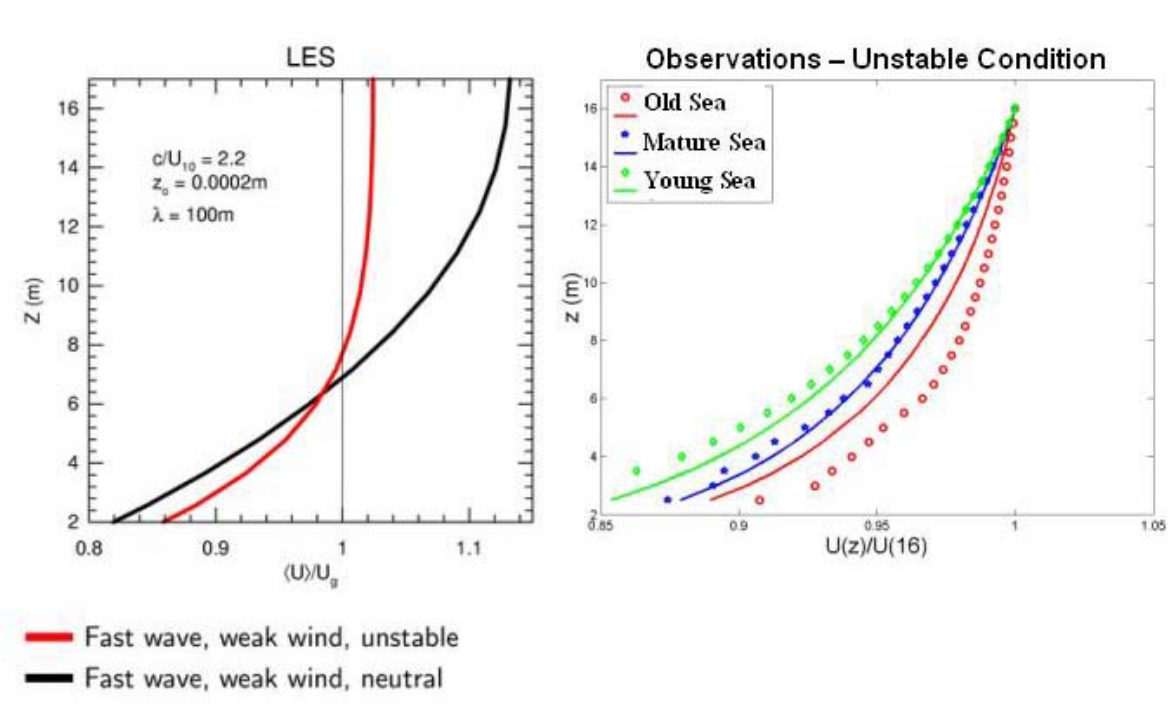

Figure 12. The left panel shows results from two of the LES runs for winds over swell in unstable and neutral conditions. The right panel shows measured (symbols) and MO predicted (lines) velocity profiles average over 3 wave age classes denoting young, mature, and old seas.

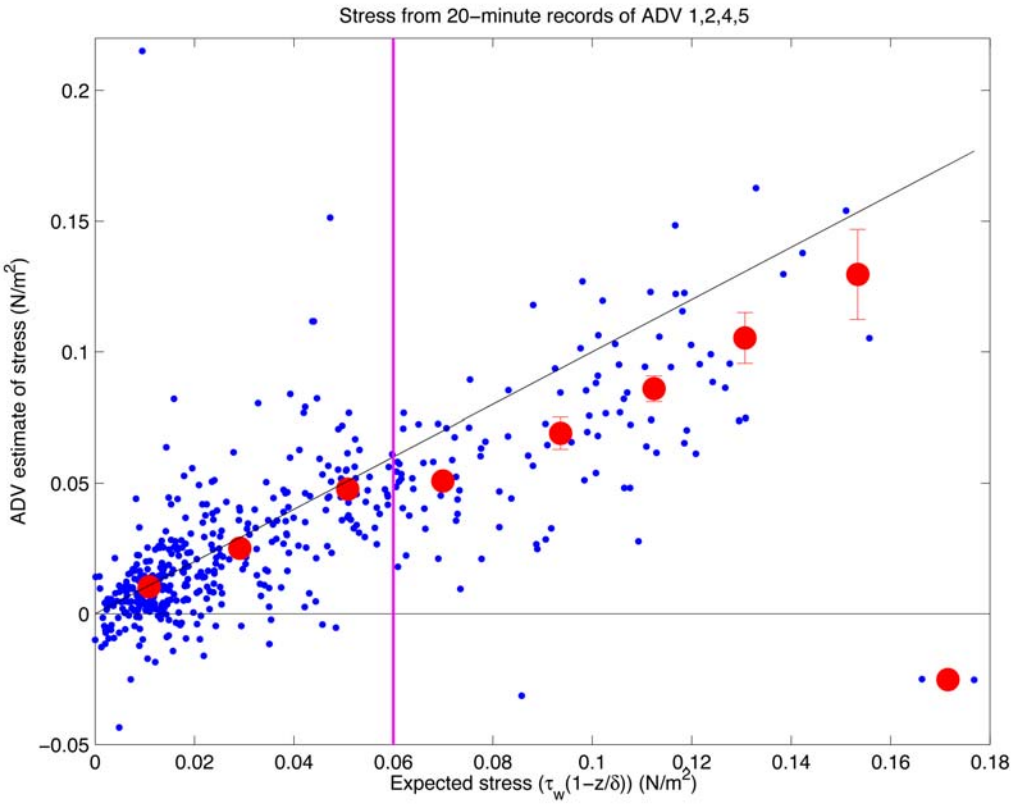

Figure 13. Comparison of subsurface stress estimates from direct covariance measurements (ADV) versus a simple mixed-layer model (expected). The red dots indicate bin-averaged results. The vertical line demarcates stresses measured at wind speeds above (to the right) and below (to the left) 7 ms^{-1}.

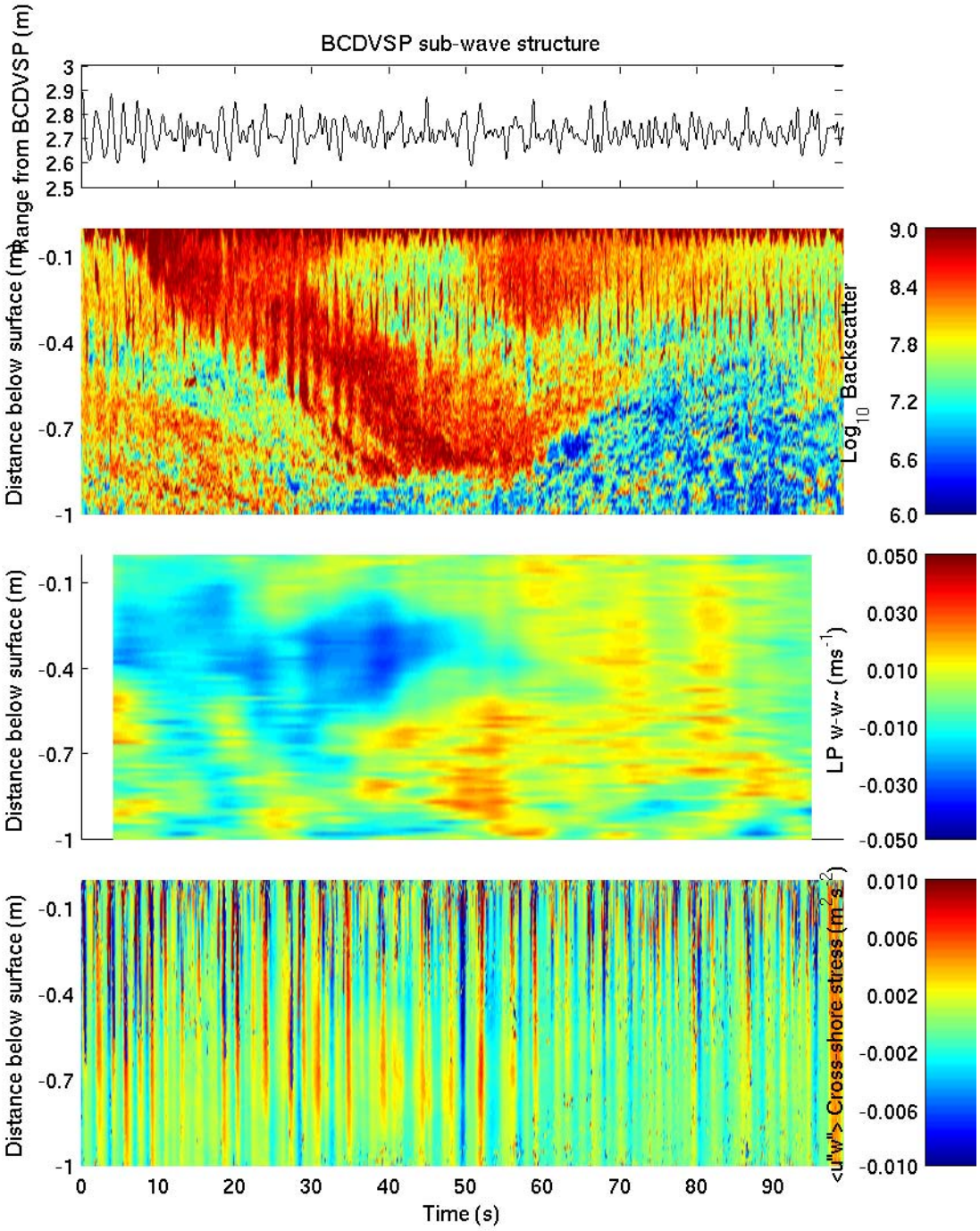

Figure 14. A 100 second profile timeseries of a.) surface elevation, b.) acoustic backscatter levels, c.) low pass filtered vertical velocity and d.) u'w' stress component correlations measured under short period, limited fetch wind waves. Bubbles injected during a wave breaking event at t=7 seconds were entrained by a sub-surface circulation cell seen in the vertical velocity profiles that have the wave-period motions filtered out. The results have been mapped into a surface-following coordinate system

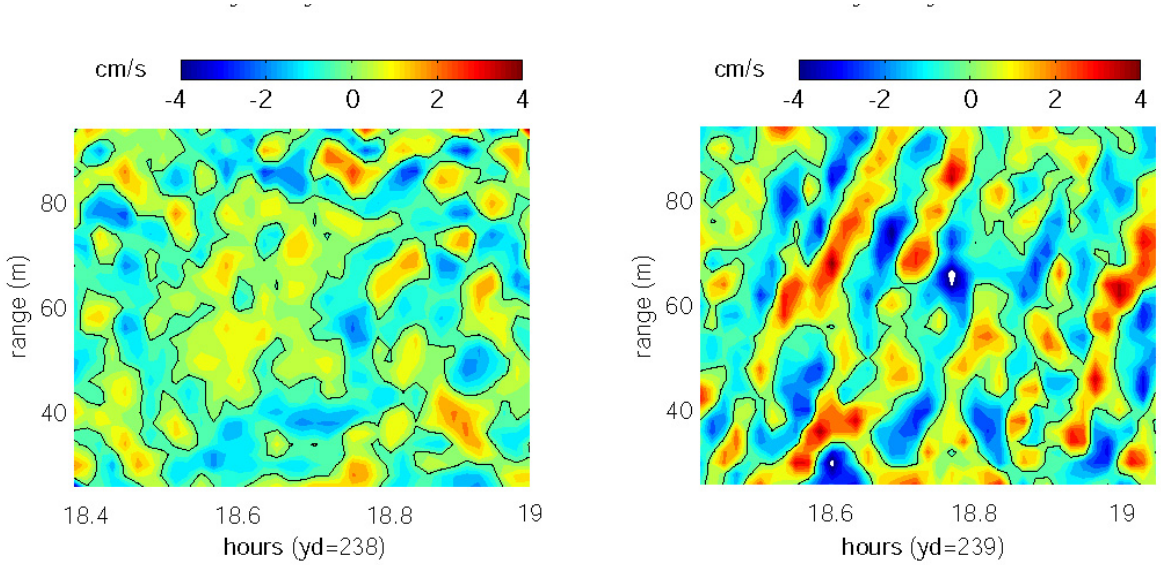

Figure 15. Time-range plots of water velocity at the sea surface based on fanbeam ADCP measurements during CBLAST-LOW. The wind speed was approximately the same during the two periods shown. However, the waves were fetch-limited and smaller in the left panel and from the open ocean and larger in the right panel.

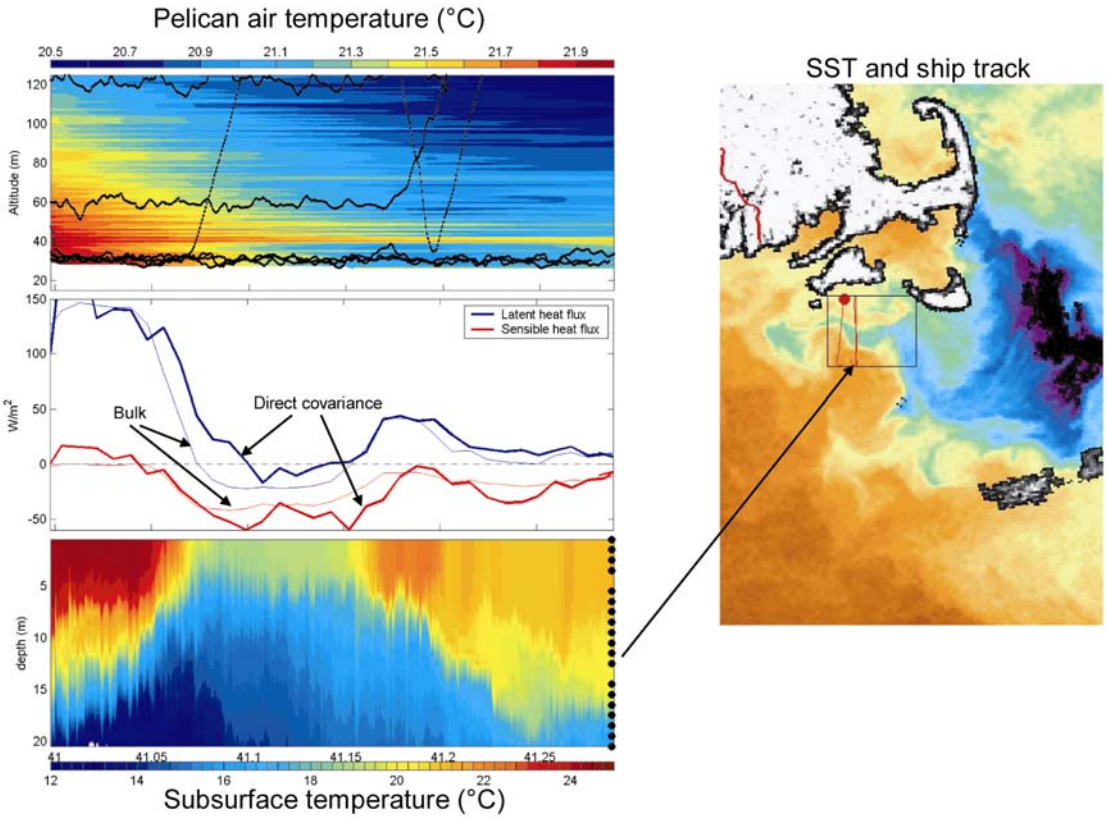

Figure 16. On the left, subsurface thermal structure (lower), sensible and latent surface heat fluxes (middle), and atmospheric temperature from the Pelican aircraft (upper) associated with the ship track shown on the right executed by the *FV Nobska* on the afternoon of August 19, 2003. The response of the atmospheric boundary layer to the SST field is evident, but the strong spatial variation of heat fluxes also affects the subsequent evolution of the SST field.

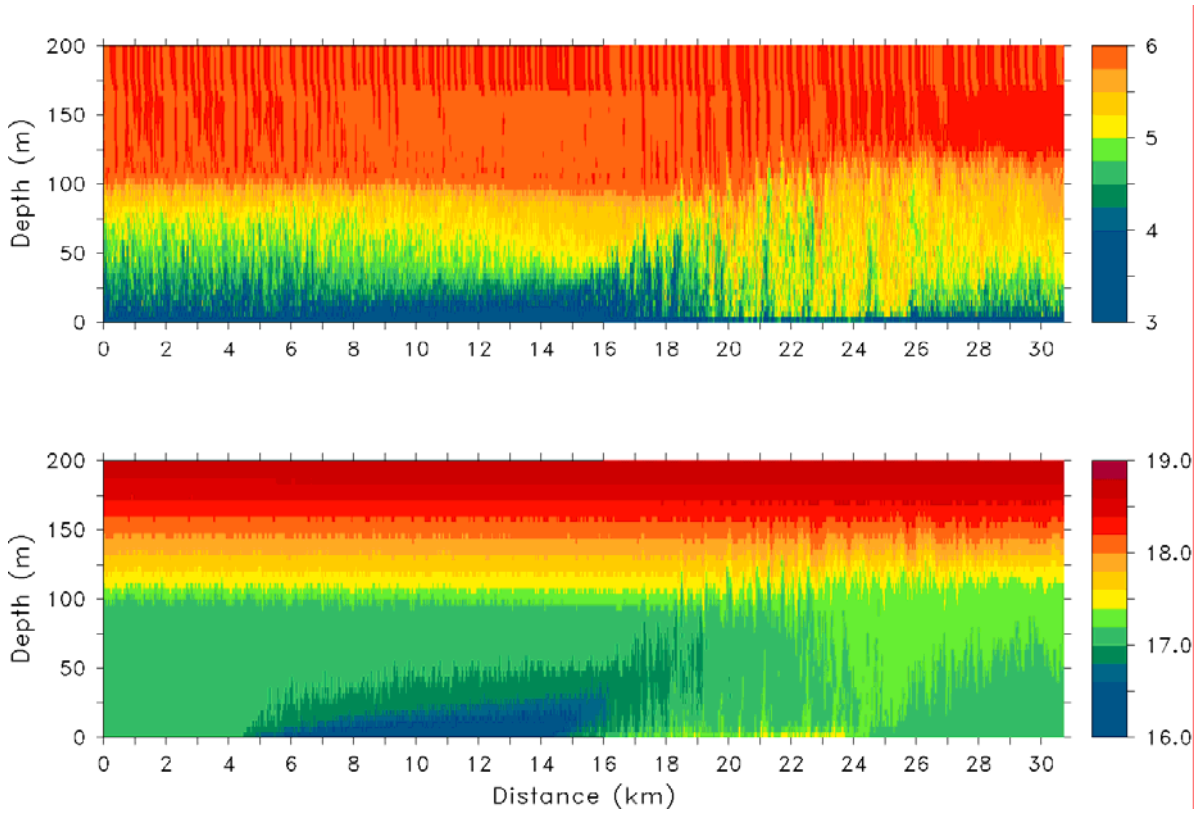

Figure 17. Cross section plots in the vertical and horizontal direction showing (a) horizontal velocity (m s^{-1}), and (b) potential temperature (^{o}C). Surface temperatures are 18 ^{o}C in Zone 1, 16 ^{o}C in Zone 2, 20 ^{o}C in Zone 3, and 18 ^{o}C in Zone 4, and the wind is from the left. The simulations indicate that the response of the atmospheric boundary layer to these small-scale SST variations would be difficult to parameterize because the boundary layer response depends on whether flow is from warm to cold water or vice-versa.

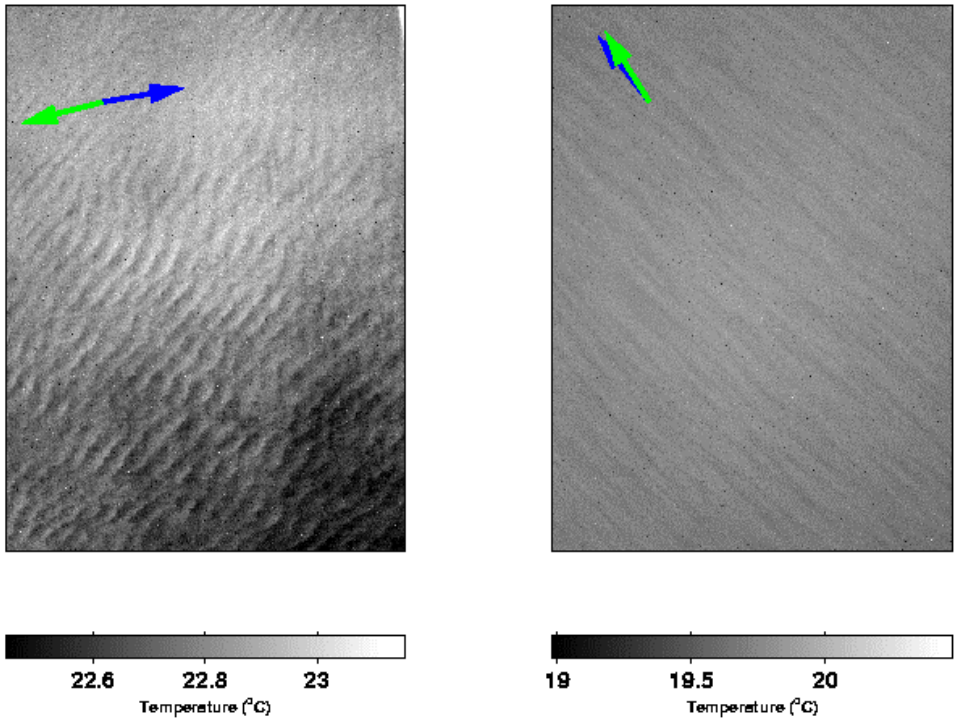

Figure 18. Left: IR image showing coherent ramp structures observed on August 14, 2003 in the afternoon. The wind speed (Blue Arrow) is roughly 4 m s^{-1} from the West and the surface current (Green Arrow) is 17 cm s^{-1} from the East. The dominant spatial scale of the variability in temperature across these coherent ramps is 14.7 m, and they extend over several km. The fact that upper-ocean thermal stratification was breaking down at this time and that the features are roughly perpendicular to the surface current suggests that these ramp-like structures may be associated with shear instabilities. Right: IR image depicting Langmuir circulation observed on August 25, 2003 in the morning. The wind speed (Blue Arrow) is roughly 5 m s^{-1} and the surface current (Green Arrow) is 47 cm s^{-1}, both from the West-Southwest. The dominant scale between these cool bands is 21.0 m, and their orientation relative to the wind and wave directions suggests that these features are associated with Langmuir circulation.

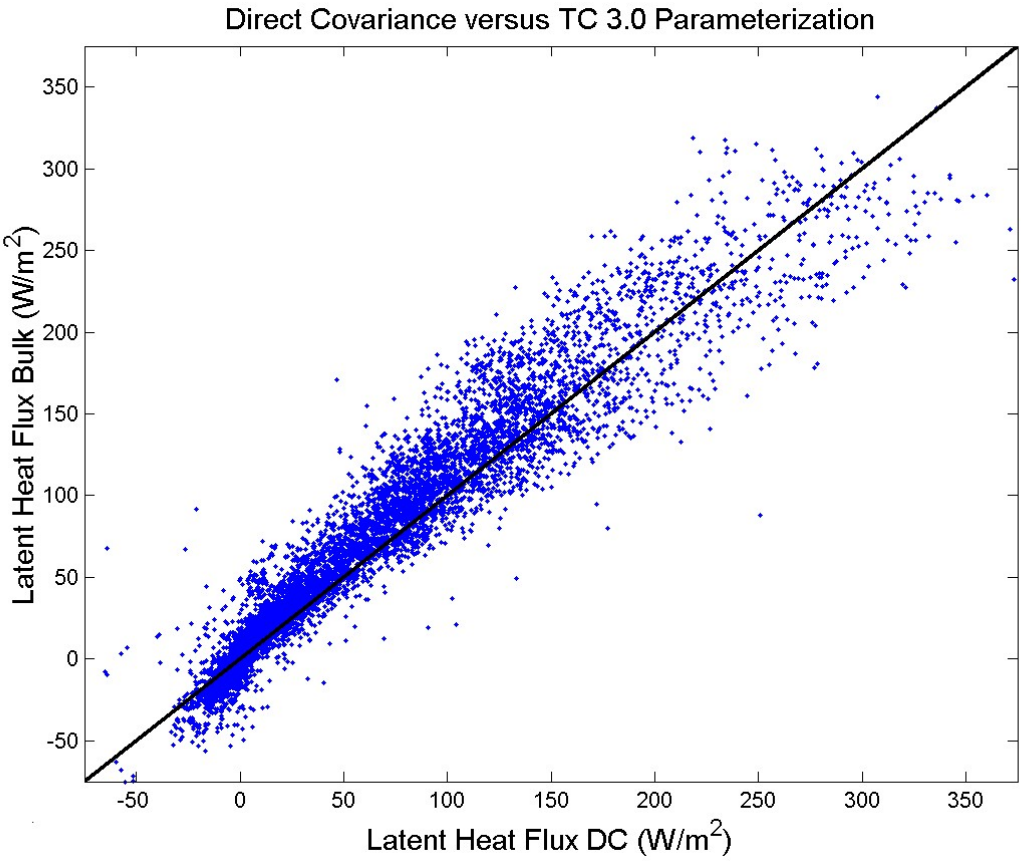

Figure 19. Comparison of direct covariance versus bulk aerodynamic latent heat fluxes measured from ASIT.

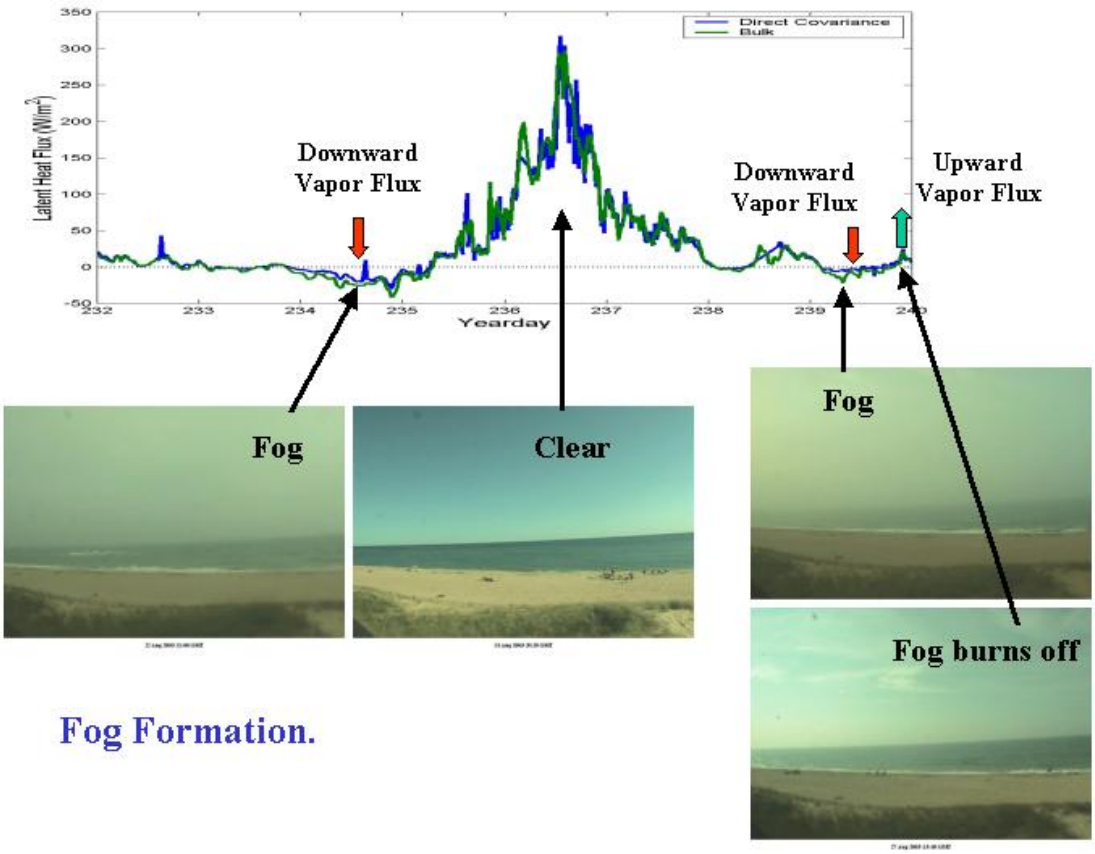

Figure 20. Time series of the latent heat fluxes and visual evidence for the presence of fog during periods of downward moisture flux.

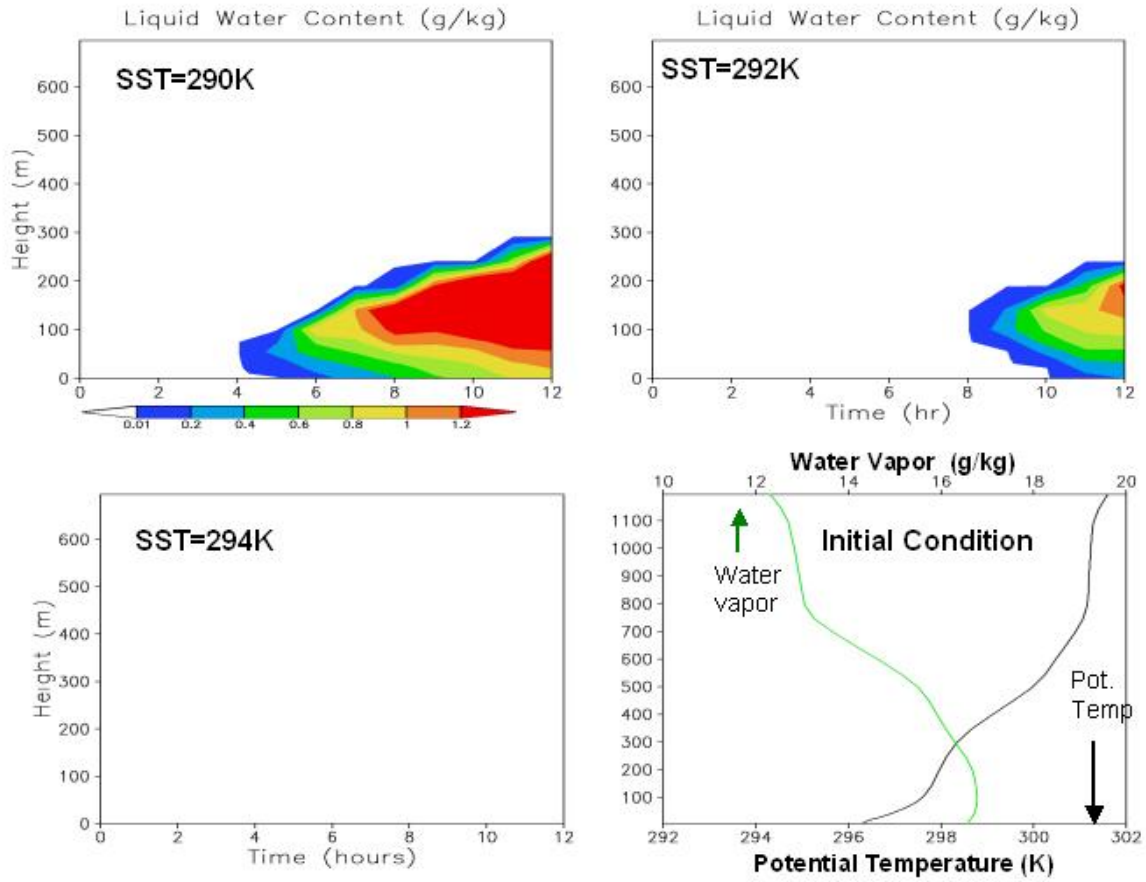

Figure 21. The sensitivity of fog formation to SST as indicted by model prediction of liquid water content.